Chemical Geology 294–295 (2012) 1–17

Contents lists available at SciVerse ScienceDirect

Chemical Geology

journal homepage: www.elsevier.com/locate/chemgeo

Magnesium and strontium systematics in tropical speleothems from the Western Pacific

Daniel J. Sinclair [a,*], Jay L. Banner [a], Frederick W. Taylor [a], Judson Partin [a], John Jenson [b], John Mylroie [c], Ethan Goddard [d], Terry Quinn [a], John Jocson [b], Blaž Miklavič [b,c]

[a] Jackson School of Geosciences, University of Texas in Austin, United States
[b] Water & Environmental Research Institute of the Western Pacific, University of Guam, Guam
[c] Department of Geosciences, Mississippi State University, United States
[d] College of Marine Science, University of Southern Florida, United States

ARTICLE INFO

Article history:
Received 24 May 2011
Received in revised form 1 October 2011
Accepted 11 October 2011
Available online 20 October 2011

Editor: J.D. Blum

Keywords:
Stalagmite
Magnesium
Strontium
Prior calcite precipitation
Incongruent calcite dissolution
Western Tropical Pacific

ABSTRACT

We present bulk average Sr and Mg data for 13 speleothems from different locations in the western equatorial Pacific (Guam, Solomon Islands, and Vanuatu). These data plot on a single straight line in a graph of ln(Sr/Ca) vs ln(Mg/Ca) with a slope of ~0.9. A 22,000 year record of Sr and Mg in one of these samples from Guam also plots with the same slope, suggesting that the process partitioning Mg and Sr *within* the Guam speleothem is the same as the one that partitions Mg and Sr *between* the different Pacific speleothems. We rule out temperature, growth rate, detrital phases, and sea-spray as likely mechanisms for this correlation. We construct mathematical models of limestone diagenesis and show that this cannot explain the slope of the correlation.

Our favoured explanation for the correlation is calcite/water interaction in the form of prior calcite precipitation (PCP) and/or incongruent calcite dissolution (ICD). We present a formal mathematical model of PCP and prove that the slope of a graph of ln(Sr/Ca) and ln(Mg/Ca) is given by $\frac{Kd_{Sr}-1}{Kd_{Mg}-1}$. A similar equation is derived for ICD in a companion paper (Sinclair, 2011). Using published values for Kd_{Sr} and Kd_{Mg}, this slope is calculated to be ~0.88, in excellent agreement with our observations. Because the slope is independent of solution and host-limestone composition it can be used to diagnose calcite–water interaction in individual cave water studies where host rock composition is unknown, or in speleothems for which no field drip water data or host-rock geochemistry exists. Approximately half of published drip and speleothem Mg + Sr studies plot within error of this slope.

We hypothesize that the overall trend in our Pacific speleothem data results from the individual dripwater systems evolving from a roughly similar initial rock composition set by late Quaternary reef limestone. In the Guam speleothem, the broad peak in Mg and Sr centred on the early–mid Holocene reflects a change in hydrology (rainfall), with the most likely scenario being that dry conditions prevailed on Guam at this time.

1. Introduction

Calcite speleothems are important climate archives. They form primarily from rainwater, and because speleothem-bearing caves can be found in many regions where permanent ice-caps are absent, they represent an important alternative to ice cores for reconstructing atmospheric and hydrological processes. Speleothem calcite can be accurately dated using the U/Th isotope system (e.g. Hellstrom, 2003), calcite is the stable polymorph at surface conditions and is thus resistant to diagenesis and open-system behaviour, and speleothems contain a number of different environmental proxies in the form of band-thickness, stable isotopes and trace elements (see reviews in Fairchild et al., 2006a; Fairchild and Treble, 2009).

Stable isotopes of oxygen ($\delta^{18}O$) are the mainstay of paleoenvironmental reconstructions from speleothems (e.g. Gascoyne, 1992). They carry a regional climate signal (Schmidt et al., 2007), and the processes controlling them are reasonably well characterised (e.g. Hendy, 1971; Bar-Matthews et al., 1996) (although Mickler et al. (2004) outlines some complexities with this proxy). Measurement of trace elements such as Mg and Sr in carbonates is now also routine (Schrag, 1999; de Villiers et al., 2002). Under the right circumstances, Mg and Sr find utility as hydrological tracers, with changes being

* Corresponding author at: Institute of Marine and Coastal Sciences, Rutgers University.
E-mail address: djsweb1971@yahoo.com.au (D.J. Sinclair).

0009-2541/$ – see front matter © 2011 Elsevier B.V. All rights reserved.
doi:10.1016/j.chemgeo.2011.10.008

linked to rainfall (Hellstrom and McCulloch, 2000; McMillan et al., 2005; Johnson et al., 2006; Cruz et al., 2007; Griffiths et al., 2010). However, these proxies are used less frequently than $\delta^{18}O$ (Cruz et al., 2007).

Some of the reluctance to use Mg and Sr derives from the large range of processes that can affect their partitioning into calcite, and the fact that many of these apply at a local level in karst systems making it more difficult to interpret records in terms of regional-scale paleoclimate. For example, the following processes have all been identified that potentially control Mg and/or Sr incorporation into speleothems: temperature, growth rate, prior calcite precipitation (PCP), dissolution of aragonite or dolomite, incongruent calcite dissolution (ICD), changes in water/rock residence time, changes in karst hydrology, cave atmosphere, marine aerosols, crystal size/geometry, soil zone processes, detrital input, etc. (e.g. Paquette and Reeder, 1995; Goede et al., 1998; Fairchild et al., 2000; Hellstrom and McCulloch, 2000; Tooth and Fairchild, 2003; Treble et al., 2003; McDonald et al., 2004; Desmarchelier et al., 2006; Fairchild et al., 2006a; Johnson et al., 2006).

A notable feature of many dripwater and speleothem geochemical studies is a positive correlation between Mg and Sr, most commonly ascribed to PCP (Fairchild et al., 2000; Tooth and Fairchild, 2003; McDonald et al., 2004; Musgrove and Banner, 2004; Fairchild et al., 2006b; Johnson et al., 2006; Karmann et al., 2007). PCP is typically diagnosed from dripwater studies by measuring and/or modelling the variation in Mg/Ca and/or Sr/Ca as a function of Ca^{2+} concentration (Fairchild et al., 2000; Tooth and Fairchild, 2003; Musgrove and Banner, 2004; Cruz et al., 2007; Partin et al., 2011; Wong et al., 2011). However, as the science of climate reconstruction from speleothems matures, and the demand for more global coverage of climate records increases, samples will increasingly be extracted from remote locations where expense and logistics may prohibit extensive dripwater sampling. In the absence of dripwater information, are there patterns of trace element behaviour in speleothems that might prove diagnostic for processes such as PCP, even without detailed knowledge of dripwater or host-rock chemistry?

Fairchild et al. (2000) recognized from their numerical modelling work that "Mg/Ca and Sr/Ca rise as calcite precipitation occurs, leading to a vector of constant slope on a log–log crossplot" [p 263], and this trend was used by McMillan et al. (2005) to identify PCP in their speleothem. However, the underlying mechanism behind the correlation, the conditions that affect the slope, whether linear behaviour is theoretically supported, and whether it is diagnostic for PCP in light of many processes which potentially co-fractionate Sr and Mg, have not been explored. In a companion paper to this, Sinclair (2011) presented theory and mathematical models of ICD showing that in some circumstances, this mechanism also predicts linear correlation between ln(Sr/Ca) vs ln(Mg/Ca) with a slope that is the same as observed for PCP.

Here we present Mg and Sr data for 13 speleothems from three islands in the Western Pacific Ocean; Guam, Solomon Islands and Vanuatu. For one of these samples (from Guam), we also present a 22,000 year time series of Mg/Ca and Sr/Ca. In this suite of speleothems we study the patterns of element correlation, placing an emphasis on the correlation between ln(Sr/Ca) and ln(Mg/Ca). We critically test our observations against the processes described above, and present calculations and mathematical proofs for PCP and limestone diagenesis mechanisms. This *mathematical* treatment allows us to formally predict the physical and chemical parameters that affect the Mg and Sr correlations (something that numerical models cannot do), which is an essential prerequisite for being able to confidently apply correlation analysis as a diagnostic tool in the absence of other field data. We then apply the correlation theory we have derived to constrain the climatic processes recorded in the Guam speleothem time series. The paleoenvironmental interpretation of the Guam record will be presented in conjunction with $\delta^{18}O$ time series in another paper (Sinclair et al., in preparation).

2. Samples and methodology

2.1. Sample collection and preparation

Eleven speleothem samples, ranging from 18 cm to 93 cm long, were collected from a number of caves in the Solomon Islands and Vanuatu in October and November of 2005. Two further samples were collected from Guam in April 2005 (Table 1, Fig. 1). Speleothem samples showed a range of colours, textures and crystallinity (Table 1), with most being partially-translucent to near opaque and white or tan in colour.

Samples were split using a diamond impregnated rock-saw cleaned in distilled water. The two halves were then polished on a series of diamond lapidary wheels (using distilled water as a polishing flux). A 10 mm thick slab was cut from one of the split halves. The polished surfaces were cleaned and thereafter handled only with gloves.

2.2. Subsampling for geochemistry

Samples were taken at 1–3 inch intervals near the growth axes of each specimen, resulting in between 10 and 30 subsamples per speleothem. These low-resolution subsamples targeted candidate regions for U/Th analyses, and therefore tended to be the most clean (white) and/or crystalline material in each specimen. Ten-milligram powder subsamples were drilled from each speleothem by hand using a dental drill with a tungsten carbide drill bit. Subsampling was carried out in a HEPA-filtered clean hood. Before and between each sample, the bit was cleaned in dilute quartz-distilled HCl, 18 MΩ deionised water, and ethanol.

The 'Big Guam' speleothem (referred to as 'Shakey' in Fig. 1 of Partin et al., 2011) was selected for generating a century-resolution time-series and an age model was assigned based on 14 U/Th dates (for full details see Sinclair et al., in preparation). 180 samples were drilled using a computer-controlled mill from a region spanning approximately 22 ka to present. Each sub-sample was 1.0 mm wide by 2.0 mm deep by 2.0 mm long resulting in 10 mg of powder. Sampling was continuous, which eased recovery of milled powder, and prevented possible aliasing in the record.

2.3. Analysis for trace elements

Powders from the low resolution subsampling were analysed for Mg, Sr, Ca by solution ICP-MS at the University of Texas in Austin following standard methods for groundwater analysis. Approximately 5 mg splits of the powder were dissolved in quartz-distilled 2% HNO_3 and diluted to a final Ca concentration of approximately 200 ppm. ^{24}Mg, ^{43}Ca, ^{88}Sr were measured on an Agilent 7500CE quadrupole mass spectrometer, with ^{45}Sc, ^{89}Y, ^{133}Cs, ^{165}Ho and ^{169}Tm added online as internal standards.

Unknown solutions were run in sequence, with one sample in 5 being a bulk drift monitor solution made from a chunk of the Suku-1 stalagmite (see below). A suite of blanks, check standards, and calibration solutions was run twice daily. Primary standardisation was carried out using mixed element solutions prepared from single element calibration solutions. These had nominal concentrations of 100 ppt, 200 ppt, 1 ppb, 2.5 ppb, 10 ppb, and 100 ppb for many trace elements. Six further high-concentration standards were made up to bracket Ca and Mg concentrations. These had Ca concentrations of 1.6 to 180 ppm, and Mg concentrations of 0.8 to 10 ppm. Calibration was checked by analysis of NIST 1640 and NIST 1643e natural (river) water standards, and an in-house check standard made from single element standards. Linearity in the ICP-MS response was verified by analysing a serial dilution of the drift monitor solution with Ca concentrations ranging from ~1 to ~400 ppm. There was no evidence for effects of matrix-strength on trace-element concentration, with the average deviation from linearity less than 1% across all dilutions.

Table 1
Speleothem samples.

sample name	Abbreviation	Sample cave	Approx. age of host limestone[a]	Lat	Long.	Altitude	Notes
Vanuatu							
Big Taurius	BT	Cave near Taurius village	500–700 ka	15°31′ S	167°01′ E	250 m	55 cm long stalagmite sampled from gallery 6 m above cave floor. Somewhat rough outside texture. White opaque interior with subtle bands of higher crystallinity. Occasional thin brown bands.
Taurius	T	Cave near Taurius village	500–700 ka	15°31′ S	167°01′ E	251 m	61 cm long stalactite fallen from roof. Found sitting on mud on cave floor — may have fallen recently. Material is white and moderately opaque.
Long Translucent	LT	Cave near Taurius village	500–700 ka	15°31′ S	167°01′ E	252 m	32 cm long stalactite found broken amidst rubble on cave floor. Smooth exterior, highly crystalline Interior with broad bands defined by changes in colour from white to brown and occasional fine opaque bands.
Short Translucent	ST	Cave near Taurius village	500–700 ka	15°31′ S	167°01′ E	253 m	21 cm long fragment of ribbon stalactite, found broken amidst rubble on cave floor. Smooth exterior, highly crystalline interior with some alternating bands of brown opaque material.
Collapse Cave	CC	Small cave beside new forest road	500–1000 ka	15°22′ S	166°58′ E	589 m	23 cm long x 19 cm wide stumpy stalagmite sampled from a cave recently opened by bulldozer. White, moderately translucent material with regions of high crystallinity and subtle fine banding.
Fapon	FP	Long cave near Fapon village	500–750 ka	15°19′ S	166°58′ E	370 m	69 cm long stalagmite sampled in gallery 4 m above river. Possible periodic inundation with river water. Moderately smooth exterior, white opaque interior with occasional discoloured bands.
Valampil	VP	Cave near Valampil village	500–750 ka	15°22′ S	167°01′ E	384 m	39 cm long stalagmite sampled from ~2 m above river level. Periodic inundation with river water likely. Smooth exterior but somewhat convoluted growth form. White opaque material.
Solomon Islands							
Forestry Cave	FC	Cave near forestry camp, Mt Austin.	250–500 ka	09°29′ S	159°58′ E	135 m	72 cm long, thick stalagmite broken recently by vandalism. White cauliflower-like texture, opaque with subtle bands of higher crystallinity.
Suku 1	S1	Suku Cave, Small Ngella Island	3500–5700 ka	09°08′ S	160°20 E	~150 m	93 cm long double 'broomstick' stalagmite sampled from side passage in long river cave. Smooth exterior with brown colouration. Frequent inundation by river likely. Material is opaque with frequent bands defined by both higher crystallinity and brown opaque detritus-rich bands.
Suku 2	S2	Suku Cave, Small Ngella Island	3500–5700 ka	09°08′ S	160°20 E	~150 m	61 cm long double 'broomstick' stalagmite sampled from side passage in long river cave. Sample has broken and started re-growing. Smooth exterior with brown colouration. Frequent inundation by river likely. Material is opaque with frequent bands defined by both higher crystallinity and brown opaque detritus-rich bands.
Suku 3	CM	Suku Cave, Small Ngella Island	3500–5700 ka	09°08′ S	160°20 E	~150 m	18 cm stumpy cave-mushroom sampled from ~1.5 m above river. Frequent river inundation likely. Mostly opaque with occasional bands of crystalline material. Frequent periodic fine banding defined by alternating brown and white layers.
Guam							
Big Guam	BG (aka 'Shakey')	Jinapsan Cave: near Jinapsan Point, N Guam.	1800–2000 ka or 116–135 ka	13°38′ N	144°53′ E	25 m	60 cm long parallel-sided stalagmite sampled ~16 m from cave entrance. Exterior is smooth. Inside, the sample ranges from very crystalline at the top, moderately crystalline in the middle, and semi-opaque near the base. Sample colour changes from dark grey to tan. Material is somewhat porous towards the periphery. Fine but irregular banding is visible throughout defined by subtle changes in crystallinity.
Small Guam (aka Stumpy)	SG (aka 'Stumpy')	Jinapsan Cave: near Jinapsan Point, N Guam.	1800–2000 ka or 116–135 ka	13°38′ N	144°53′ E	25 m	35 cm long parallel-sided stalagmite sampled ~16 m from cave entrance. Exterior is smooth. Inside the sample is moderately crystalline, light tan in colour. Irregular banding is visible throughout defined by changes in crystallinity.

[a] Dates for Vanuatu and Solomon Islands limestones are based on cave altitudes and dates/uplift rates published in Taylor et al. (2005) and Chen et al. (2011). The age of the Guam limestone is based on the work of Miklavič (2011). Jinapsan cave is hosted in the Plio-Pleistocene Mariana Limestone, but is overlain by Tarague Limestone identified as MIS 5e, (with dates from Stirling et al. (1998) and Esat et al. (1999)). The Florida Island limestone (Suku Cave) is Miocene in age based on nannofossil biostratigraphy (N-zone N17-N19/20; see Hughes, 1989).

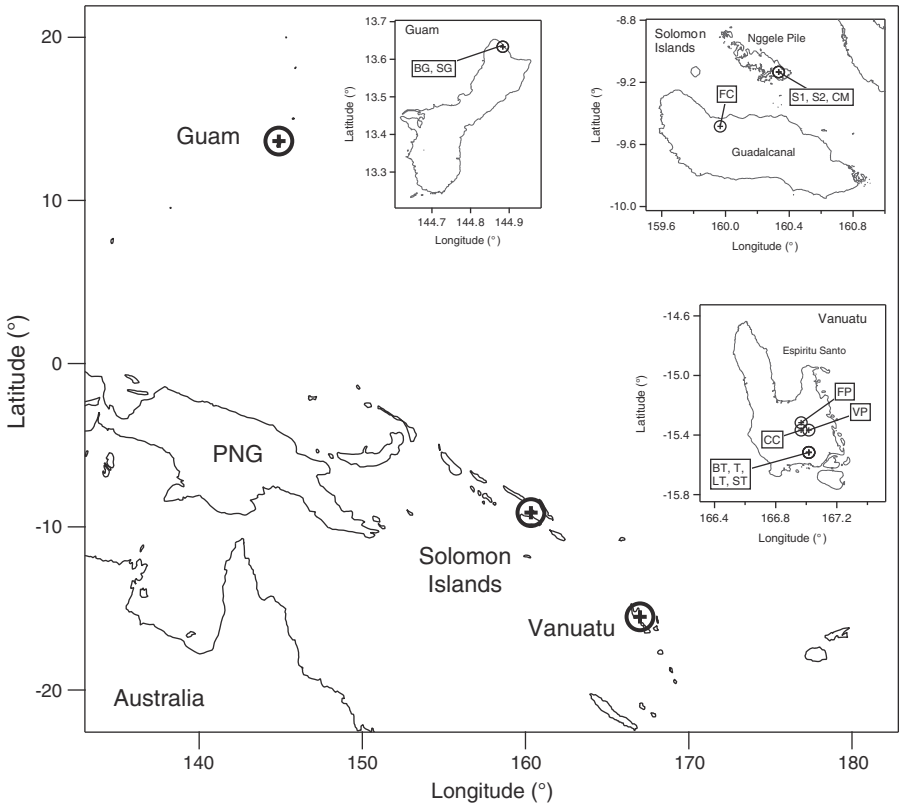

Fig. 1. Sample locations. Samples were collected from Guam, the Solomon Islands (islands of Guadalcanal and Nggele Pile), and Vanuatu (island of Espiritu Santo). Tags indicate locations of individual samples, referencing the abbreviations listed in Table 1.

After blank subtraction, correction to internal standards, and calibration using the primary solution standards, the reproducibility of the drift monitor analyses (over six separate days of ICP-MS analysis) was 3% for Mg, 2% for Ca, and 2% for Sr (1σ for n = 63). A secondary drift-correction was applied by linear interpolation between the drift monitor solutions. This reduced the reproducibility to 0.8% for Mg, 0.8% for Ca, and 1.1% for Sr (1σ, estimated from 60 paired/multiple replicates of standards and/or unknown solutions over the six days of analysis).

Estimates of accuracy vary for each standard, and was best in the case of the check standard, perhaps because it was prepared from the same stock solutions as the primary calibration solutions. The average difference between known and measured concentrations was 2% for Mg, 1% for Ca, and 1% for S (n = 12 analyses). Accuracy for measurements of NIST 1643e (n = 11) was 1% for Mg, 5% for Ca, and 3% for Sr. Accuracy for measurements of NIST 1640 (1σ, n = 13) was 5% for Mg, 15% for Ca, and 2% for Sr.

Powders from the Guam speleothem century-resolution time-series were analysed for Sr and Mg at the University of South Florida by ICP-OES using a method modified from Schrag (1999). Measurements were made on a Perkin Elmer 4300 DV Inductively Coupled Plasma-Optical Emission Spectrometer. Analytical precision for Sr/Ca and Mg/Ca determinations, based on repeated measurements of a gravimetric standard is ±0.22% (2σ; ±0.0025 mmol/mol) and ±0.21% (2σ; ± 0.0069 mmol/mol), respectively. The standard used to calibrate the Sr/Ca and Mg/Ca data has been externally verified by TIMS at the University of Minnesota Isotope Laboratory (Sr/Ca) and ICP-MS at the University of California, Santa Barbara (Mg/Ca).

3. Results

3.1. Guam stalagmite

Trace element data for the Guam speleothem high-resolution time series are presented in Fig. 2. The Mg/Ca and Sr/Ca data are plotted against age in Fig. 4a and b (see Sinclair et al., in preparation for details of the age model). The Sr/Ca and Mg/Ca time series are both characterised by a large amplitude peak centred approximately 12 cm from the top of the speleothem. This results in a significant correlation between these elements in both linear (Fig. 2) and logarithmic (Fig. 3) plots. The slope of the ln(Sr/Ca) vs ln(Mg/Ca) correlation is 0.96 ± 0.12 (Table 2). The non-peak data are excluded from this correlation because of a systematic drift in the Mg/Sr, which shows a steady increase from approximately 14 ka until present and may be driven by another mechanism (see Sections 4.3.1 and 4.3.4).

3.2. Suite of Pacific stalagmites

The Mg/Ca and Sr/Ca data for the suite of Pacific speleothems are presented in Fig. 3. Only about half of the speleothems show significant Sr/Ca vs Mg/Ca correlations; however, the bulk averages for each speleothem form a strong positive correlation when graphed as ln(Sr/Ca) vs ln(Mg/Ca) (Fig. 3). One cluster of speleothems – all from the Taurius cave in Vanuatu – plot slightly above this trend. The overall slope of the ln(Sr/Ca) vs ln(Mg/Ca) correlation is 0.70 ± 0.24 if the Taurius samples are included, and 0.85 ± 0.16 if the Taurius samples are excluded (Table 2). The slope of the trend is very similar to the slope observed for the Mg and Sr peak in the Guam stalagmite (Fig. 3).

3.3. Survey of published dripwater and speleothem studies

To test whether the mechanism fractionating Mg and Sr in our speleothems is an expression of a universal mechanism, we summarize published data where Mg and Sr have been measured on the same samples in Tables 2 and 3. The slopes of studies yielding positive correlations between ln(Sr/Ca) and ln(Mg/Ca) are listed in Table 2 and graphed in Fig. 5. Data is presented only where it

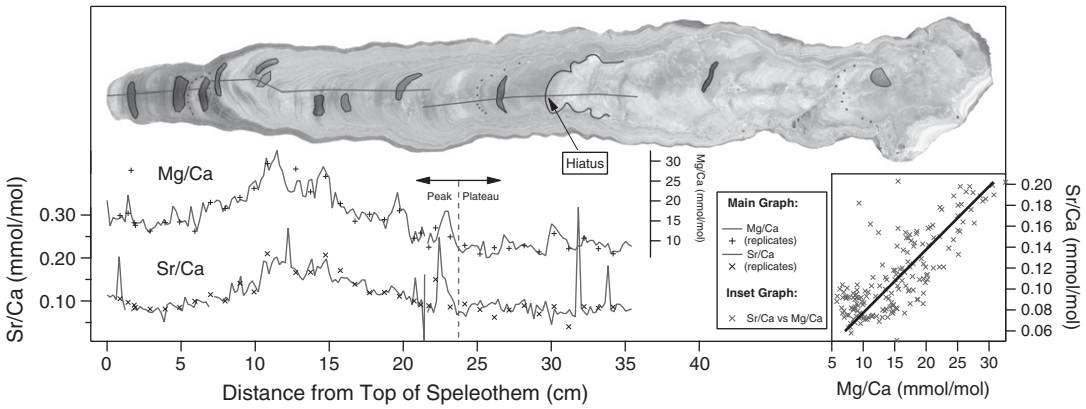

Fig. 2. Mg/Ca and Sr/Ca profiles for the Guam speleothem. Dark regions on the speleothem image represent the locations of U/Th dates (see Sinclair et al., in preparation). Note the broad peak centred on the first 1/3 of the speleothem record. For correlation analysis (Fig. 3), the data have been divided into two regions: the flat (plateau) portion, and the peak. Inset graph: Sr/Ca vs Mg/Ca showing the linear correlation.

has been possible to extract Mg/Ca and Sr/Ca data from the tables/figures published. While this is not an exhaustive survey, it serves to illustrate the range of correlation behaviour observed, and the degree to which other cave systems show correlations similar to the Pacific speleothems. Approximately half of the water sites and speleothems examined have positive ln(Sr/Ca) vs ln(Mg/Ca) slopes that are within error of those observed for the Pacific speleothems.

4. Discussion

The key result of this study is the observation that the bulk average Mg/Ca and Sr/Ca ratios in speleothems from different caves in different islands separated by considerable distances (>3500 km) all plot along one linear trend. This is a surprising result, implying that a single geochemical process has first-order control over the bulk composition of all these speleothems. On a log–log plot, this trend

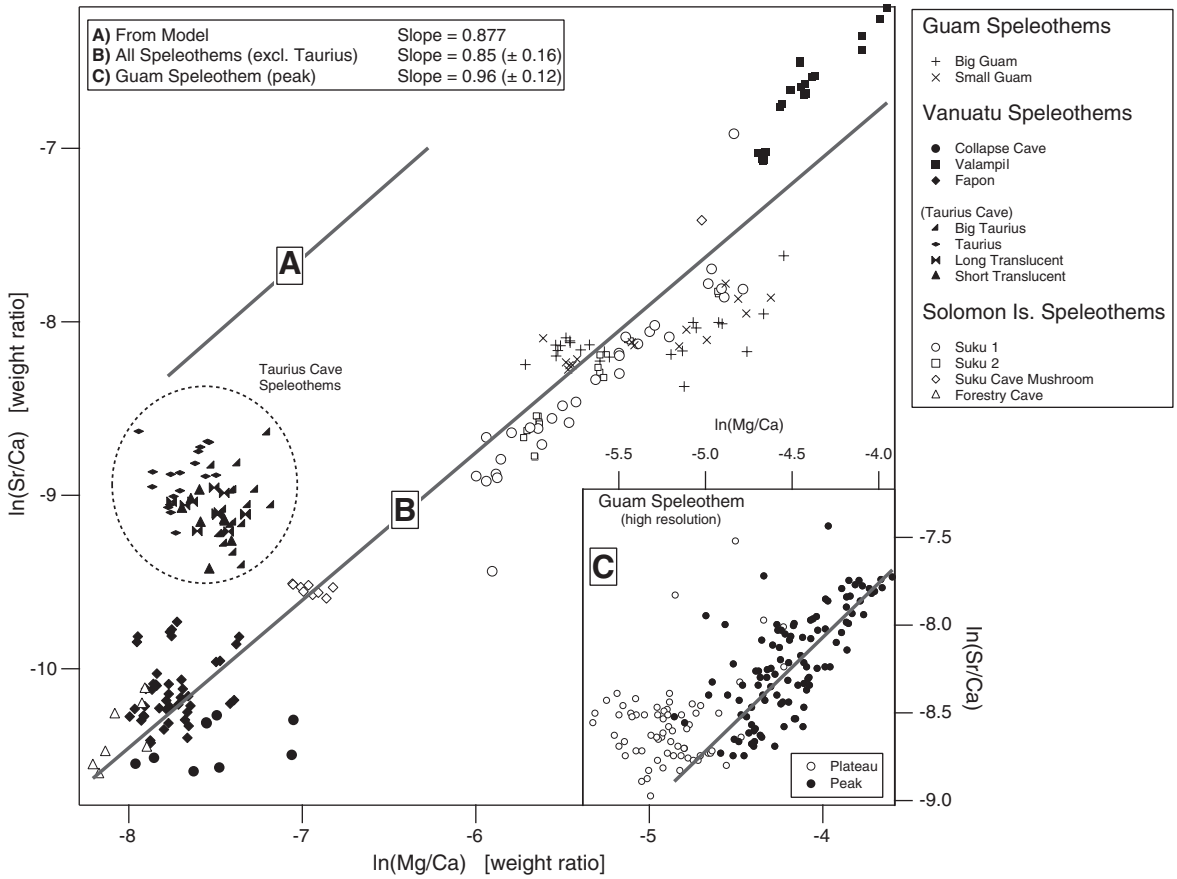

Fig. 3. ln(Sr/Ca) vs ln(Mg/Ca) for all Pacific speleothems. Main graph: filled symbols are speleothems from Vanuatu. Open symbols are speleothems from the Solomon Islands. Cross symbols are speleothems from Guam. Line A shows the theoretical slope predicted for PCP and ICD (see text). Line B is the linear fit through all the speleothem data excluding Taurius Cave (where dissolution of aragonite-rich casts elevates Sr values). Inset graph: filled symbols are data for the peak-region of the high-resolution Guam dataset. Open symbols are data from the plateau-region of the profile (see Fig. 2). Line C is the linear fit to the peak-region of the profiles. Note that the axes of the inset graph are scaled such that slopes are directly comparable to the main graph.

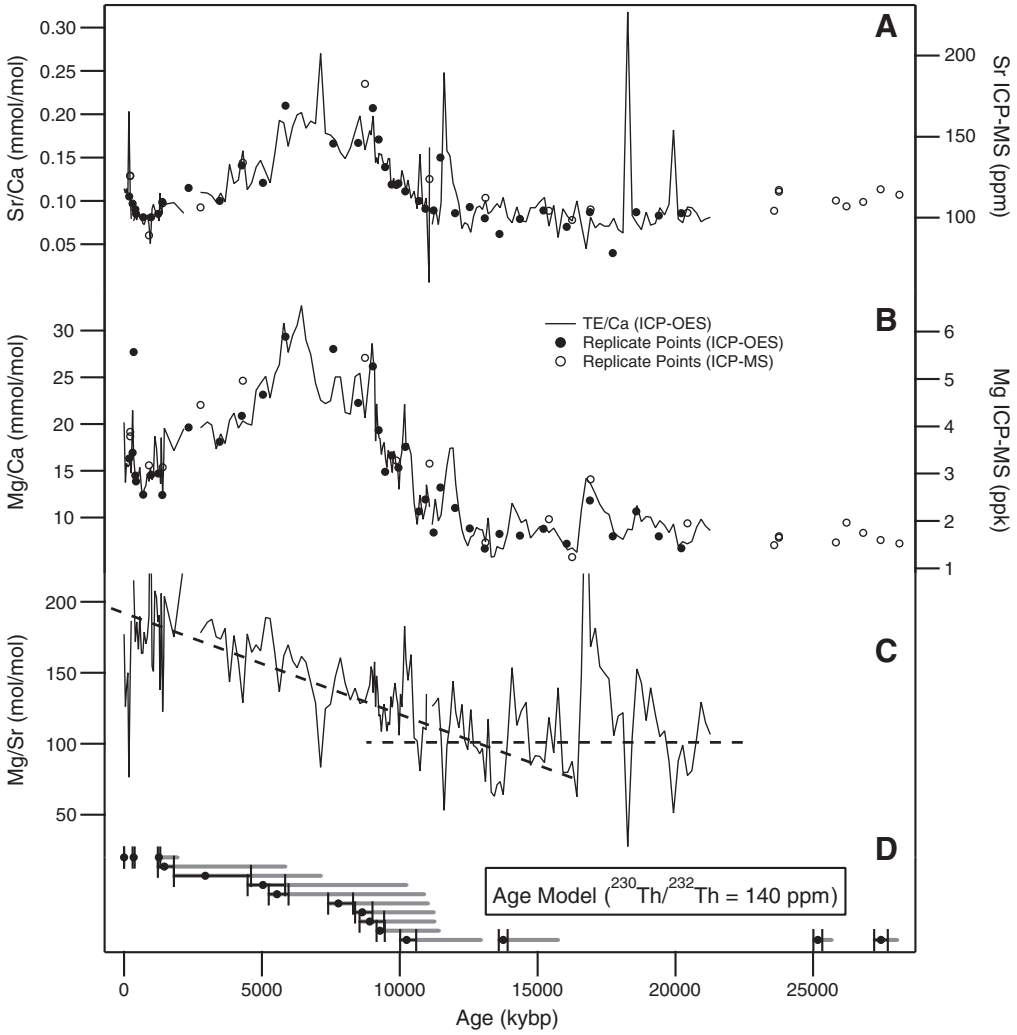

Fig. 4. Multiple tracers in the Guam speleothem. A: Sr/Ca in the Guam speleothem. The line is the century-resolution analysis by ICP-OES. The solid circles are duplicate points milled just adjacent to the original transect. The open circles are ICP-MS analyses from the low-resolution survey. B: Mg/Ca in the Guam speleothem. See A: for further details. C: Mg to Sr ratio as a function of time. Note the increase beginning around 13–15 ka. The lines indicate the approximate trends with time. D: Preferred age model for the Guam speleothem (see Sinclair et al., in preparation for more details). The model assumes a constant ^{230}Th/^{232}Th ratio and imposes a monotonic age constraint. The error bars represent the age range permissible (^{230}Th/^{232}Th ratios between 135 and 147 ppm). The grey bars represent the maximum and minimum age bounds assuming a variable ^{230}Th/^{232}Th ratio (see Sinclair et al., in preparation for more details).

has a slope of ~0.85 (Fig. 3), which is the same (within error) as Mg and Sr variations *within* the Guam speleothem (Figs. 2 and 3) and many other speleothem/drip-water systems (Fig. 5). This suggests that the same process can operate at local scales within an individual dripwater system, as well as on a regional scale. In the following discussion we investigate potential mechanisms that might produce a linear ln(Sr/Ca) vs ln(Mg/Ca) relationship with the observed slope.

Excepting the cases where the Mg and Sr respond to growth processes and/or come from contaminant phases in the speleothem (Sections 4.3.1 and 4.3.2), a trend in stalagmite composition ultimately derives from variations in the drip waters. Bedrock can impose primary control over karst-water Mg and Sr composition (e.g. Karmann et al., 2007; Fairchild and Treble, 2009), with subsequent water/rock interactions (including diagenesis) potentially modifying this composition. Thus, two general mechanisms can be envisaged which might be responsible for co-fractionating the Sr and Mg in the dripwaters: *Mechanism 1* (modification of dripwaters): karst waters begin with approximately similar Mg and Sr contents (implying host limestones have a broadly similar composition), and the trend observed in Fig. 3 derives from differing degrees of subsequent modification of those karst waters by water–rock interaction upstream of the drip site. *Mechanism 2* (limestone diagenesis): karst waters primarily reflect the composition of their host limestones, and the trend arises because these limestones have systematically evolved different bulk Mg + Sr compositions through different degrees of diagenetic modification.

We consider modification of dripwaters in Section 4.1, where we examine prior calcite precipitation (Section 4.1.1) and incongruent calcite dissolution (Section 4.1.2). We study limestone diagenesis in Section 4.2 where we investigate dissolution of unstable minerals in limestone (Section 4.2.1), and the behaviour of Mg and Sr during cycles of dissolution/reprecipitation of calcite in an open system (Section 4.2.2). In Section 4.3 we also investigate whether temperature, precipitation rate, detrital phases, soils and sea-spray input are plausible mechanisms for the Mg and Sr co-fractionation.

4.1. Modification of dripwaters by calcite water interactions

4.1.1. Prior calcite precipitation (PCP)

Prior calcite precipitation is one of the most often cited explanations for a positive correlation between Mg and Sr seen in drip-waters and speleothems (Fairchild et al., 2000; Huang et al., 2001; Tooth and

Table 2
Observed ln(Sr/Ca) vs ln(Mg/Ca) correlation slopes.

Observation	Slope of correlation	Graph ref
This paper		
Guam Speleothem Flat Region	0.26 ± 0.3	1
Guam Speleothem Peak	0.96 ± 0.12	2
All Pacific Speleothems (no exclusions)	0.70 ± 0.24	3
All Pacific Speleothems (excluding Taurius Cave)	0.85 ± 0.14	4
PCP and ICD Theory 'Most Likely' Scenario (see Table 3)	0.877 to 0.973	Dark grey
PCP and ICD Theory Max and Min Scenarios (see Table 3)	0.709 to 1.003	Light grey
McGillen and Fairchild (2005): incongruent dissolution experiments		
Experiment D	0.99	5
Experiment E	1.23	6
Experiment H	1.27	7
Experiment J	0.73	8
Experiment T	0.88	9
Average	1.02 ± 0.23	10
Cruz et al. (2007) and Karmann et al. (2007) Brazilian Cave dripwaters		
Bt2 Stalagmite	1.16 ± 0.21	11
Pool 1	0.95 ± 0.25	12
Drip 1	0.94 ± 0.29	13
Pool 2	0.82 ± 0.10	14
Drip 2	0.92 ± 0.19	15
Drip 3	0.94 ± 0.24	16
Musgrove and Banner (2004): Texas Cave waters		
Inner Space Caverns, Press Room Drip	0.82 ± 0.4	17
Inner Space Caverns, Flowing Stone of Time Pool + Cascade + Discovery Room	0.82 ± 0.08	18
Inner Space Caverns, Lake of the Moon Drip	0.96 ± 0.1	19
Inner Space Caverns, Flowing Stone of Time Drip	0.3 ± 0.1	20
Inner Space Caverns, Lake of the Moon Rim Pool	0.37 ± 0.07	21
Natural Bridge Caverns, All waters	0.52 ± 0.04	22
McDonald et al. (2004): East Australian Cave dripwaters		
K2 Drip Site	1.0 ± 0.3	23
K2 Drip Site	0.87 ± 0.17	24
	0.93 ± 0.12	25
K1 and K2 combined.		
Buhl et al. (2007): Moroccan Speleothem		
Aoufous Stalagmite	1.13 ± 0.19	26
Huang et al. (2001): Grotta di Ernesto		
S1 Pool	0.75 ± 0.35	27
G5 Pool	−0.3 ± 0.9	28
G3 Drip	0.62 ± 0.48	29
G1 Drip	−0.3 ± 0.9	30
Combined Pools	0.86 ± 0.21	31
All Cave Waters	0.69 ± 0.26	32
Stalagmite ER76	0.41 ± 0.05	33
Soda Straw	Negative	
Fairchild et al. (2000): Grotta di Ernesto		
First Chamber Drips + Pools	1.67 ± 0.54	34
Main Chamber Drips + Pools	0.73 ± 0.45	35
Fairchild et al. (2006b): Brown's Folly Mine dripwaters		
Drip F5	1.3 ± 0.5	36
Drip B		37
Drip F1		38
McMillan et al. (2005): Grotte de Clamous speleothem		
Stalagmite CL26c	1.13 ± 0.14	39
Fairchild et al. (2001): Irish stalagmite		
Ballynamintra Cave sample BA99-4	0.21 ± 0.09	40
Griffiths et al. (2010): Flores, Indonesia stalagmite		
Liang-Luar Cave sample LR06-B1	1.6–2.2[a]	41
Wong et al. (2011): Natural Bridge Caverns dripwaters		
Group 1 (PCP)	0.87 ± 0.03	42
Group 3 (mixed PCP and water–rock interaction)	0.67 ± 0.03	43
Partin et al. (2011): Jinapsan Cave dripwaters		
All Drips	0.79 ± 0.09	44
Johnson et al. (2006): Heshang Cave, China, stalagmite		
HS-4 Solution ICP-MS Data	0.76 ± 0.21	45

[a] Variable slope along speleothem. Note — noise in data quantified using methodology in Sinclair et al. (2005, 2011) then decimated to optimal resolution before correlation analysis.

Table 3
Survey of Sr/Ca vs Mg/Ca correlations in the literature.

Study	Location	Cave	Sample ID	Type	Slope within error of PCP slope?	Comments
This paper	Northwest Tropical Pacific, Guam	Jinapsan Cave	Big Guam	Stalagmite	Yes	Peak only (see text)
This paper	Northwest Tropical Pacific, Guam	Jinapsan Cave	Small Guam	Stalagmite	Yes	Peak only (see text)
This paper	Western Tropical Pacific, Vanuatu	Valampil Cave	Valampil	Stalagmite	Yes	
This paper	Western Tropical Pacific, Vanuatu	Collapse Cave	Collapse Cave	Stalagmite	No	No correlation
This paper	Western Tropical Pacific, Vanuatu	Fapon Cave	Fapon	Stalagmite	No	No correlation
This paper	Western Tropical Pacific, Vanuatu	Taurius Cave	Taurius	Stalactite	Yes	Subset of record
This paper	Western Tropical Pacific, Vanuatu	Taurius Cave	Big Taurius	Stalagmite	Yes?	Slope very uncertain (few data points)
This paper	Western Tropical Pacific, Vanuatu	Taurius Cave	Short Translucent	Stalactite	No	Negative correlation
This paper	Western Tropical Pacific, Vanuatu	Taurius Cave	Long Translucent	Stalactite	No	No correlation
This paper	Western Tropical Pacific, Solomon Is.	Forestry Camp Cave	Forestry Cave	Stalagmite	Yes	
This paper	Western Tropical Pacific, Solomon Is.	Suku Cave	Cave Mushroom	Stalagmite	No	Negative correlation
This paper	Western Tropical Pacific, Solomon Is.	Suku Cave	Suku 1	Stalagmite	Yes	
This paper	Western Tropical Pacific, Solomon Is.	Suku Cave	Suku 2	Stalagmite	Yes	
Partin et al. (2011)	Western Tropical Pacific, Guam	Jinapsan Cave	All Drips	Drip	Yes	
Hellstrom and McCulloch (2000)	New Zealand, South Island	Nettlebed Cave	MD3	Flowstone	No	Negative Correlation
Desmarchelier et al. (2006)	Southeast Australia, Tasmania	Frankcombe Cave	FC-SS5	Soda-straw	No	Negative correlation
McDonald et al. (2004)	Eastern Australia	Kooringa Cave	K1	Drip	Yes	
McDonald et al. (2004)	Eastern Australia	Kooringa Cave	K2	Drip	Yes	
Treble et al. (2003, 2005)	Southwest Australia	Moondyne Cave	MND-S1	Stalagmite	No	Negative correlation
Cruz et al. (2007)	Southern Brazil	Botuverá Cave	Bt2	Stalagmite	Yes	
Karmann et al. (2007)	Southern Brazil	Santana Cave	TSE	Pool	Yes	
Karmann et al. (2007)	Southern Brazil	Santana Cave	EE2, EE1	Drip	Yes	
Karmann et al. (2007)	Southern Brazil	Santana Cave	TIF, EIF, TSF	Pool	Yes	
Karmann et al. (2007)	Southern Brazil	Santana Cave	ESF	Drip	Yes	
Karmann et al. (2007)	Southern Brazil	Santana Cave	FR	Drip	Yes	
Griffiths et al. (2010)	Flores, Indonesia	Liang-Luar Cave	LR06-B1	Stalagmite	No	Slope variable, but in general much steeper.
Ku and Li (1998)	Northeastern China	Shihua Cave	S312	Stalagmite	No	No correlation
Johnson et al. (2006)	Southern China	Heshang Cave	HS-4	Stalagmite	Yes	
McGillen and Fairchild (2005)	UK and Switzerland	Limestones	(various)	Leaching experiments	Yes	Slopes measured between high and low pCO_2 experiments
Roberts et al. (1999)	Southwest UK	GB Cave	GB-91-1, GB-91-2, GB91-MC-2.2	Stalagmites	No	No correlation
Fairchild et al. (2006b)	Southern UK, Bath	Brown's Folly Cave	F5	Drip	Yes	Slope not well constrained
Fairchild et al. (2006b)	Southern UK, Bath	Brown's Folly Cave	B	Drip	No	Slope Too Shallow
Fairchild et al. (2006b)	Southern UK, Bath	Brown's Folly Cave	F1	Drip	No	No correlation
Roberts et al. (1998)	Northern Scotland	Tartair Cave	SU80-11	Stalagmite	No	No correlation (negative correlation in places)
Fairchild et al. (2001)	Northwest Scotland	Tartair Cave	SU96-7	Stalagmite	No	Negative correlation
Fairchild et al. (2001)	Southeast Ireland	Ballynamintra Cave	BA99-4	Stalagmite	No	Slope too shallow
Fairchild et al. (2001)	Southwest Ireland	Crag Cave	CRAG-R	Soda-straw	No	Negative correlation

Table 3 (*continued*)

Study	Location	Cave	Sample ID	Type	Slope within error of PCP slope?	Comments
Fairchild et al. (2001)	Belgium	Pere-Noël Cave	PN26	Calcite coating	No	No correlation
Fairchild et al. (2001)	Northeast Italy	Ernesto Cave	ER77	Stalagmite	No	No Correlation
Borsato et al. (2007)	Northeast Italy	Ernesto Cave	ER78	Stalagmite	No	No Correlation (Negative Correlation at Lower Frequencies)
Huang et al. (2001)	Northeast Italy	Ernesto Cave	ER76	Soda-Straw	No	Negative Correlation
Huang et al. (2001)	Northeast Italy	Ernesto Cave	ER76	Stalagmite	No	Slope Too Shallow
Huang et al. (2001)	Northeast Italy	Ernesto Cave	S1, G5, G3	Pools + Drip	Yes	
Huang et al. (2001)	Northeast Italy	Ernesto Cave	G1	Drip	No	No Correlation
Fairchild et al. (2000)	Northeast Italy	Ernesto Cave	First Chamber Drip + Pools	Waters	No	Too Steep (but slope uncertain)
Fairchild et al. (2000)	Northeast Italy	Ernesto Cave	Main Chamber Drip + Pools	Waters	Yes	
Fairchild et al. (2000)	Southern France	Clamouse Cave	Grand Carrefour	Drip	No?	Too Steep (but slope uncertain)
Fairchild et al. (2000)	Southern France	Clamouse Cave	Couloir Blanc	Drip	No?	Too Steep (but slope uncertain)
Fairchild et al. (2000)	Southern France	Clamouse Cave	C12 Drip	Drip	No?	Too Steep (but slope uncertain)
Fairchild et al. (2000)	Southern France	Clamouse Cave	Salle de Gour Sec	Drip	Yes?	Slope very uncertain (few data points)
Fairchild et al. (2000)	Southern France	Clamouse Cave	C2 Drip	Drip	Yes?	Slope very uncertain (few data points)
Mattey et al. (2008)	Southern Spain, Gibralter	New St Michaels Cave	Gib04a	Stalagmite	Yes	
Huang and Fairchild (2001)	Inorganic Experiments	Laboratory	Plates 3,6,11 Straw 46, 49	(Artificial) Straws and Plates	No	Negative correlation
Musgrove and Banner (2004)	Central Texas	Inner Space Caverns	Press Room Drip	Drip	Yes	
Musgrove and Banner (2004)	Central Texas	Inner Space Caverns	Flowing Stone of Time Pool + Cascade + Discovery Room	Waters	Yes	
Musgrove and Banner (2004)	Central Texas	Inner Space Caverns	Lake of the Moon Drip	Drip	Yes	
Musgrove and Banner (2004)	Central Texas	Inner Space Caverns	Flowing Stone of Time Drip	Drip	No	Slope too shallow
Musgrove and Banner (2004)	Central Texas	Inner Space Caverns	Lake of the Moon Rim Pool	Pool	No	Slope too shallow
Musgrove and Banner (2004)	Central Texas	Natural Bridge Caverns	All waters	Waters	No	Slope Too Shallow
Wong et al. (2011)	Central Texas	Natural Bridge Caverns	Group 1 (PCP)	Drip	Yes	Very tightly constrained.
Wong et al. (2011)	Central Texas	Natural Bridge Caverns	Group 3 (mixed PCP and calcite recrystallization)	Drip	No	Slope too shallow. Consistent with mixture of PCP and calcite recrystallization.
Buhl et al. (2007)	Northwest Africa, Morocco	Aoufous Cave	Aoufous Speleothem	Stalagmite	Yes	

Fairchild, 2003; McMillan et al., 2005; Fairchild et al., 2006b; Johnson et al., 2006; Cruz et al., 2007; Mattey et al., 2008) and we favour this mechanism to explain the Mg and Sr trends observed in this study. Because the partition coefficients for Mg and Sr in calcite are lower than unity, Mg/Ca and Sr/Ca ratios in a solution precipitating calcite become progressively enriched and subsequently-precipitated calcite will be co-enriched in Mg and Sr. This is essentially a case of Rayleigh fractionation, and recent numerical models have shown that Rayleigh fractionation is consistent with trace element partitioning in some stalagmites (e.g. Johnson et al., 2006).

Fairchild et al. (2000) note that PCP results in a vector of constant slope in log–log plots of Sr/Ca vs Mg/Ca. However, no slope is given, and no explanation is advanced for the apparent universality of this relationship. Numerical models (computational simulations) do not offer further insights so we have therefore constructed a *mathematical* model (formal derivation of formulae) describing PCP to study the behaviour of the system. Full derivation and equations for the model are presented in Electronic Appendix A.

If we assume that partition coefficients are constant and that PCP is the only process occurring in a closed water/rock system, then

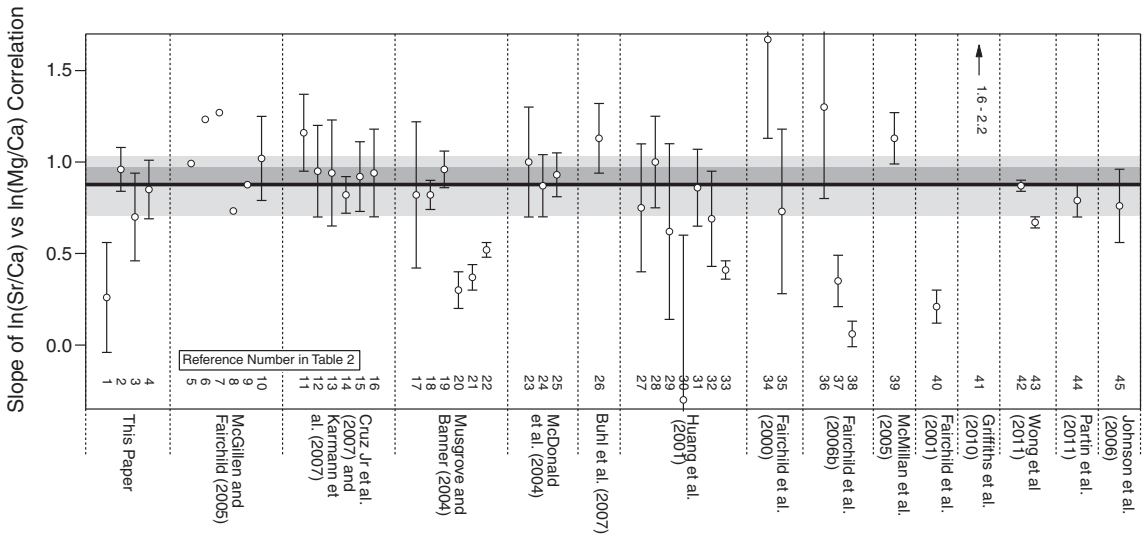

Fig. 5. Slopes of ln(Sr/Ca) vs ln(Mg/Ca) correlations for published stalagmite and dripwater studies. The correlation slopes are graphed with 95% confidence intervals determined from linear fitting to the data. Numbers along the bottom of the graph refer to reference numbers in Table 2. The light grey band represents the maximum range of slopes predicted for calcite–water interaction (PCP and ICD) based on published values of Kd_{Sr} and Kd_{Mg} (see text and Tables 4 and 5). The dark band represents the 'most likely' range for the predicted slope, while the black line represents our preferred value.

cave waters evolving under PCP, and speleothems forming from them, will display a positive linear correlation between ln(Sr/Ca) vs ln(Mg/Ca), which has a slope given by $\frac{Kd_{Sr}-1}{Kd_{Mg}-1}$ (see Equations A9 and A10 in the derivations presented in Appendix A). A similar relationship was derived by Gagnon et al. (2007) expanding on the equations of Elderfield et al. (1996) to explain element partitioning in aragonite during coral biomineralization. This trend is a universal property of PCP, and is *independent of both host-rock and solution composition*. The slope potentially changes slightly if Kd_{Sr} and Kd_{Mg} vary with local conditions (see below for discussion), but will otherwise be the same for any karst system in the world. The slope applies equally for both cave waters and speleothem forming from them. Thus, this slope is very useful for diagnosing PCP, even when there has been no characterization of dripwaters or host rock.

Using the values for Kd_{Sr} and Kd_{Mg} reviewed in Banner (1995) and Huang and Fairchild (2001) (see Table 4), we calculate a maximum range of possible PCP slopes from 0.709 to 1.003 (Table 5). This can be constrained further: a slope > 1.0 is unlikely as this implies that $Kd_{Sr} < Kd_{Mg}$ whereas the opposite is generally accepted. Huang and Fairchild (2001) measured Kd_{Mg} at 25 °C of 0.031. Since this is very close to the annual average temperature at Guam (26 °C), we adopt this estimate for our 'most likely' scenario. Huang and Fairchild measured Kd_{Sr} under karst-analogue conditions and obtained values of 0.057 to 0.078, which they acknowledge is lower than published field measurements (which average around 0.15). Our 'most likely' scenario therefore uses Kd_{Sr} of 0.057 to 0.15. Our selected Kds give ln(Sr/Ca) vs ln(Mg/Ca) slopes of 0.88–0.97 with the lower estimate being preferred as this is in accord with field measurements (Table 5). The slope we observe for both the Guam speleothem and the suite of Pacific speleothems is identical, within error, to this range. Thus, PCP is a strong candidate for the mechanism responsible for the correlations seen in Fig. 3.

Because Kd_{Mg} is sensitive to temperature, and Kd_{Sr} to growth rate (see review in Section 4.3.1), the value of $\frac{Kd_{Sr}-1}{Kd_{Mg}-1}$ would be sensitive to both. However, since $Kd_{Mg} \ll 1$, $(Kd_{Mg}-1) \approx -1$, and hence the numerical value of $\frac{Kd_{Sr}-1}{Kd_{Mg}-1}$ is primarily determined by the value of $(Kd_{Sr}-1)$ (Gagnon et al., 2007). The predicted PCP slope is therefore highly *in*sensitive to temperature. A 4 °C warming such as might have occurred during the glacial-interglacial transition would result in a ~0.7% increase in slope. The growth rate dependence of Kd_{Sr} (Section 4.3.1) would be expected to

Table 4
Kd summaries presented in Huang and Fairchild (2001).

KdSr	Note	Citation
0.057–0.078	Experiments	Huang and Fairchild, 2001
0.13–0.2 (bulk)	Lorey Caves Virginia	Holland et al., 1964
0.13–0.23 (bulk)	Vancouver Island	Gascoyne, 1983
0.09–0.30 (bulk)	Jamaica	Gascoyne, 1983
0.15–0.16 (micro)	N Italy	Huang et al., 2001
0.15 (bulk)	W Ireland	Huang and Fairchild, 2001 (citing data presented in Fairchild et al., 2001)
KdMg	**Note**	**Citation**
0.017–0.027[a]	(Seawater) experiments	Mucci and Morse (1983)
0.030 ± 0.005	Experiments	Howson et al. (1987)
0.031	Experiments at 25 °C	Huang and Fairchild (2001)
0.019	Experiments at 15 °C	Huang and Fairchild (2001)
0.014	Field data at 5 °C	Huang et al. (2001)
0.013–0.06	Various[b]	Various[b]

[a] Values change depending on Mg/Ca ratio.
[b] Range presented in Huang and Fairchild (2001) Figure 11.

Table 5
Calculations of ln(Sr/Ca) vs ln(Mg/Ca) slopes using different combinations of partition coefficients from Table 4.

KdSr	KdMg	$\frac{(Kd_{Sr}-1)}{(Kd_{Mg}-1)}$
0.057	0.06	1.003
0.057	0.031	0.973 [a]
0.15	0.031	0.877 [a]
0.3	0.019	0.714
0.3	0.013	0.709

[a] 'Most likely' scenarios.

result in a 3.5–7.0% decrease in $\frac{Kd_{Sr}-1}{Kd_{Mg}-1}$ for an order of magnitude faster growth.

We note that this partitioning theory is applicable for any pair of elements that substitute for Ca in calcite with a constant partition coefficient, allowing additional tests for PCP behaviour.

4.1.2. Incongruent calcite dissolution (ICD)

Incongruent calcite dissolution is another potential calcite/water interaction which could fractionate Mg and Sr relative to Ca. Dissolution of calcite – especially from fresh surfaces – is often incongruent, with both Sr and Mg being released in preference to Ca (Land, 1967; Schroeder, 1969; Reeve and Perry, 1994; Fairchild et al., 2000; McGillen and Fairchild, 2005).

Sinclair (2011) developed two mathematical models to study Mg and Sr partitioning during ICD. Both models represent kinetic dissolution/recrystallization scenarios within closed systems. The first model is based on the assumption that ICD represents congruent dissolution of a metastable $CaCO_3$ with simultaneous reprecipitation of a secondary calcite with a composition dictated by the solution composition and the partition coefficients for Mg and Sr. The second model is based on the assumption that within a thin layer of calcite at a freshly exposed surface, Mg, Sr and Ca dissolve into solution while all the time maintaining constant partition coefficients. This model represents ion leaching from mobile sites in the crystal, and simulates the short-lived 'burst' of Mg and Sr that is often observed after the exposure of fresh calcite surfaces (e.g. Fairchild et al., 1994; Fairchild and Killawee, 1995; Fairchild et al., 1999; McGillen and Fairchild, 2005).

Both ICD models predict that the slope of a ln(Sr/Ca) vs ln(Mg/Ca) graph varies with time, but that under circumstances which might prevail in karst systems, the curves approach linearity with slopes given by $\frac{Kd_{Sr}-1}{Kd_{Mg}-1}$ (Sinclair, 2011). This is an identical result to the slope predicted for PCP, and just as with PCP, this limiting slope is a constant universal property of the ICD system, independent of host rock or solution composition. Since the calculated slope (~0.88) is a close match to our observed slope, ICD is also a candidate for the process generating the Mg and Sr correlations in Fig. 3.

4.2. Diagenesis

If the bulk limestone composition imparts a first-order control over dripwater composition, then diagenetic changes to the Mg and Sr content of limestone could account for the trend between different speleothems seen in Fig. 3. We do not favour this explanation because there is no correlation between stalagmite Mg + Sr and host limestone age (Fig. 6). This is most clearly demonstrated in the Suku cave speleothems which have grown from the same host limestone, yet plot with bulk Mg values which differ by more than a factor of 5 (Fig. 6). Clearly, hydrogeochemical processes operating on the scale of individual drips are more significant for setting the bulk Mg + Sr composition of the stalagmites than the composition of the host limestone. This does not exclude the possibility that diagenesis along individual drip pathways affects the drips, however, so in the following sections we present models of two potential diagenesis mechanisms. Ultimately these models demonstrate that diagenesis cannot explain the correlated Sr/Ca vs Mg/Ca trends we see.

4.2.1. Stabilization of mineral assemblages

Young reef limestone is composed primarily of aragonite and high-Mg calcite (Morse and Mackenzie, 1990; Moore, 2001). Under meteoric conditions these minerals dissolve rapidly, and are replaced

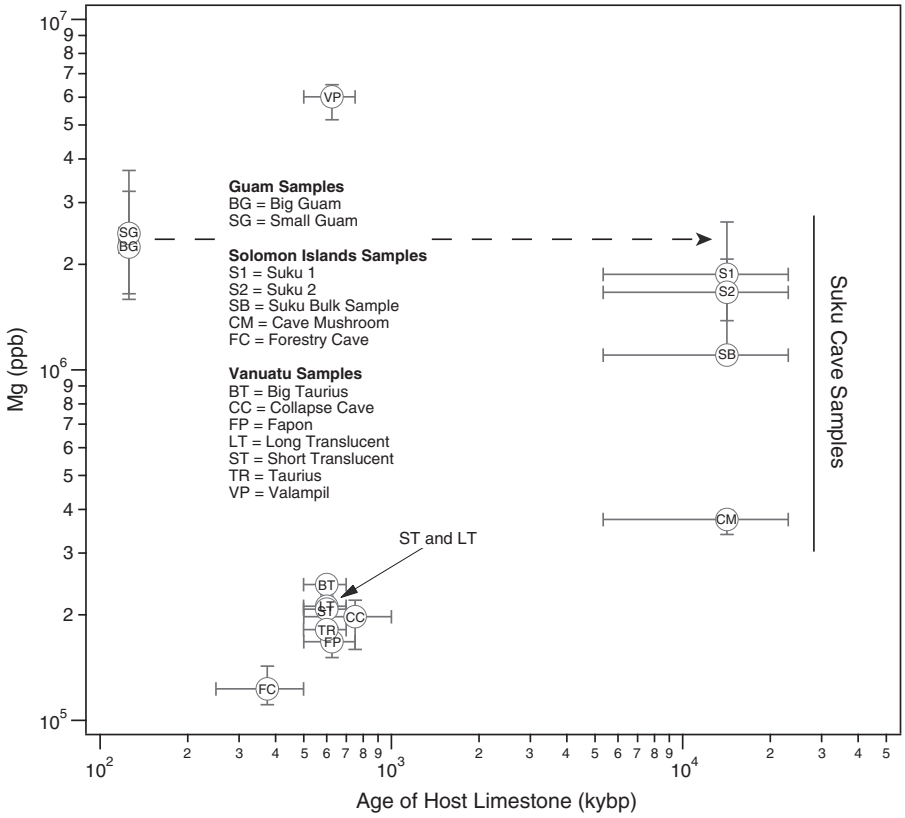

Fig. 6. Magnesium content of speleothems as a function of host rock age. Vertical error bars are the 25th–75th percentile range for the Mg content of each speleothem. Horizontal error bars give the range in estimated age for the host limestones (see Table 1 for details). Note that there is no correlation between speleothem Mg content and the age of the host limestone, as might be predicted if the host limestones were undergoing progressive diagenesis. Note also that the Suku Cave samples span a factor of 5 in Mg content. The dashed arrow indicates the two possible ages of the limestone through which the Guam speleothem dripwater may have passed (see Table 1 for details).

Table 6
Estimating minimum seawater mixing ratio necessary to account for peak in Mg/Ca and Sr/Ca in the Guam speleothem.

	Ca	Sr	Mg
Baseline ratio to Ca in speleothem	–	0.081 mmol/mol	8.4 mmol/mol
Peak ratio to Ca in speleothem	–	0.202 mmol/mol	32.7 mmol/mol
Partition Coefficient (Kd)[a]	–	0.15	0.031
Baseline ratio to Ca in dripwater[b]		0.54 mmol/mol	271 mmol/mol
Peak ratio to Ca in dripwater[b]		1.35 mmol/mol	1055 mmol/mol
Concentration in dripwater[c]	1 mM	0.54 μM	0.271 mM
Concentration in seawater[d]	10.3 mM	89 μM	53 mM
% Seawater required to reproduce peak ratio to Ca		1.1%	1.8%

[a] See text for discussion on Kds.
[b] Reconstructed using the Kd.
[c] Reconstructed from an assumed Ca concentration. The [Ca] used is a lower-bound estimate, based on the values from Tatár et al. (2004), and verified by PHREEQC calculations equilibrating calcite with pure water at present-day atmospheric pCO2.
[d] Values from Pilson (1998).

by the thermodynamically stable low-Mg calcite. Relative to low-Mg calcite, aragonite is much richer in Sr (Finch et al., 2001) while high-Mg calcite has higher Mg (Carpenter and Lohmann, 1992) (Table 7). Thus, as these minerals dissolve, they release Mg and Sr into solution resulting in a net loss from the system. With time, the Mg and Sr content of the bulk rock decreases and a positive correlation between Sr/Ca and Mg/Ca in the bulk rock could occur. Morse and Mackenzie (1990) present graphs of the bulk mineral content of Bermudian limestones (based on a study by Ristvet, 1971) showing that high-Mg calcite and aragonite contents decreased systematically during meteoric diagenesis (Figure 7.25 p 336 in Morse and Mackenzie, 1990). Using these mineral amounts, and published Sr and Mg compositions (Table 7), we model the evolution of Mg/Ca and Sr/Ca in the bulk limestone with time (Fig. 7).

Fig. 7 shows that the slope of ln(Sr/Ca) vs ln(Mg/Ca) is not constant; beginning around 0.3, and increasing rapidly as Mg/Ca and Sr/Ca decrease within the rock. This nonlinear pattern is produced because Mg-calcite dissolves faster than aragonite (Morse and Mackenzie, 1990), hence the primary source of Mg becomes depleted before the primary source of Sr resulting in an infinite slope. While there is a portion of the curve where the slope is around 0.88 (Fig. 7), this slope is maintained for only a narrow range of Sr and Mg content. The dissolution of aragonite and Mg-calcite would not produce a linear trend like the one seen in Fig. 3 where the linear relationship between ln(Sr/Ca) vs ln(Mg/Ca) is sustained over two orders of magnitude.

If dolomite was present in the system, then similar arguments apply. Like high-Mg calcite, dolomite is rich in Mg, but depleted in Sr relative to calcite (Fairchild et al., 2000; Finch et al., 2001). Dissolution of this mineral alone cannot therefore produce a positive correlation in Mg/Ca vs Sr/Ca (Frisia et al., 1997; Fairchild et al., 2000). Dolomite dissolution would need to be accompanied by aragonite dissolution, requiring a coincidental matching of dissolution rates to generate a positive correlation with the observed slope.

Although dissolution of high-Mg calcite, aragonite and dolomite are not likely the cause of the correlated Mg and Sr behaviour, it may be responsible for second-order deviations from correlated variations arising from another mechanism. For example, Mg input from dolomite dissolution will lower the slope of a ln(Sr/Ca) vs ln(Mg/Ca) plot, while Sr input from aragonite dissolution will steepen the slope. The cluster of samples from the Taurius cave, which plot above the overall Pacific Speleothem trend (Fig. 3), may have had Sr enriched by dissolution of aragonitic clasts within the coral-reef limestone.

4.2.2. Calcite recrystallization

As noted in Section 4.1, Mg and Sr are preferentially partitioned into the solution phase during calcite/water interactions. If solution is constantly percolating through limestone, dissolving and/or reprecipitating calcite as it goes, the effect will be to progressively leach Sr and Mg from the rock. We investigate this leaching using two mathematical models of an open limestone/water system in which karst water reaches equilibrium (determined by the partition coefficients) with the host rock before being removed and replaced by fresh solution. These models, their founding assumptions and mathematical derivations, are presented in full detail in Electronic Appendix C.

Both models require some degree of equilibration between limestone and solution. This is generally applicable only for a thin veneer of limestone in contact with solution where solid-state ion diffusion is potentially fast enough to allow equilibration (Stipp et al., 1996; Villegas-Jimenez et al., 2009). The models are most applicable to cases where there is a low solution volume and a large area of limestone surface. These conditions might be encountered during diagenesis of a very porous limestone and/or vadose diagenesis where solution is a thin film trickling across a large surface area of limestone (see Appendices C and D).

4.2.2.1. Model 1. The first of the two models begins with a fixed volume of limestone, and tracks its composition as it is progressively dissolved by increments of fresh water which equilibrate with the rock and are then removed from the system. This model does not allow for the exposure of new limestone as the initial limestone dissolves, and thus is most applicable at low amounts of partial dissolution where the overall volume of reactive rock has not changed much.

Model 1 (Appendix C) predicts that Mg and Sr will be co-depleted from the limestone. When ln(Sr/Ca) is graphed against ln(Mg/Ca), the model predicts the slope will be given by $\frac{(Kd_{Sr}-1)Kd_{Mg}}{(Kd_{Mg}-1)Kd_{Sr}}$. Substituting the values for Kd_{Sr} and Kd_{Mg} listed in Table 5 returns slopes of ~0.18–0.53. This range of slopes is significantly lower than the slope of 0.85 in Fig. 3. This model, therefore, does not reproduce our observations.

4.2.2.2. Model 2. Model 2 is an extension of model 1, considering the scenario where the thickness of reactive limestone stays constant so that as rock dissolves from the outside surface, the reactive layer migrates into the solid exposing new limestone. Model 2, therefore, provides a more realistic simulation of the system as leaching becomes more pronounced.

The model generates a hyperbolic relationship between ln(Sr/Ca) and ln(Mg/Ca) rather than a linear one (Fig. 7b, Appendix D). However, the function approaches linearity at low amounts of dissolution (before

Table 7
Sr/Ca and Mg/Ca in typical limestone minerals.

Mineral	Sr/Ca (mol/mol)	Mg/Ca (mol/mol)	Note
Mg-Calcite	0.00171	0.1441	Mid range value for data from Carpenter and Lohmann (1992)
Aragonite	0.00900	0.0047	Mid range value for Porites Coral from review in Sinclair et al. (1998)
Calcite	0.00023	0.0103	Enewetak Atoll Pleiocene Limestone, 100% low-Mg Calcite (Quinn, 1991)

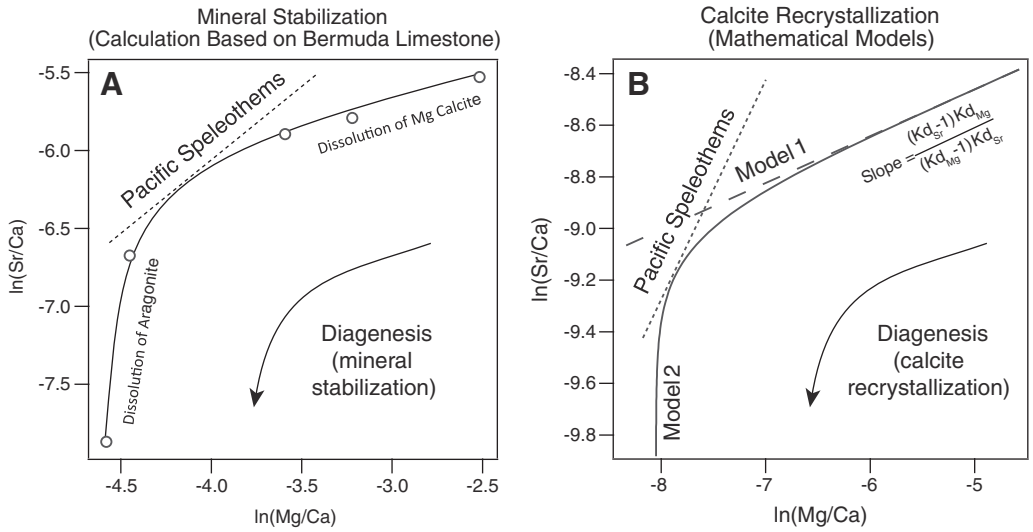

Fig. 7. ln(Sr/Ca) vs ln(Mg/Ca) in Limestones for Diagenesis Scenarios. A) Calculations for the evolution of limestones as Mg-Calcite and Aragonite transform to Calcite. Values were calculated using the mineral weight percentages from Morse and Mackenzie (1990 Figure. 7.25) and the Mg/Ca and Sr/Ca values presented in Table 7. The dashed straight line indicates the slope of the line observed in Fig. 2. Diagenesis by mineral stabilization results in progressive depletion of Mg and Sr in the limestone. The trend is highly non-linear: at the early stage of diagenesis, the rapid loss of Mg-Calcite results in a rapid decrease in Mg/Ca of the limestone. Once Mg-Calcite is depleted, the change in limestone composition is dominated by the loss of aragonite resulting in a rapid decrease in Sr/Ca. B) Mathematical models for the evolution of calcite during open-system recrystallization using equations presented in Appendix D, and values listed in Tables 5 and 7. The fine dashed straight line indicates the slope of the line observed in Fig. 2. The heavy dashed straight line is the output of Model 1 (the simplified model) while the unbroken line is the output of Model 2. The trend in Model 2 is highly non-linear but at early stages of diagenesis it approximates a straight line. The increase in slope results from Mg-depletion in the calcite.

there has been significant depletion of ions from the reactive layer) with a slope given by $\frac{(Kd_{Sr}-1)Kd_{Mg}}{(Kd_{Mg}-1)Kd_{Sr}}$. Thus for partial leaching, the slope of a plot of ln(Sr/Ca) vs ln(Mg/Ca) approaches that derived for Model 1. Again, this limiting slope is significantly shallower than observed in Fig. 3. As more Sr and Mg are removed from the reactive layer, the slope of the function approaches infinity, producing the hyperbolic shape of the function seen in Fig. 7b. Although there is a region where the slope will be 0.88, this slope is maintained over only a very narrow range of Mg/Ca and Sr/Ca values, and could not produce the extended straight-line relationship spanning several orders of magnitude that is observed in Fig. 3.

Neither model reproduces an extended linear correlation between Mg/Ca and Sr/Ca with a slope of ~0.88. Thus we conclude that diagenesis by calcite recrystallization cannot account for the observed trend in Mg and Sr in the suite of Pacific speleothems.

4.3. Other possible mechanisms

4.3.1. Temperature and growth rate

We can rule out temperature being responsible for the Mg/Ca and Sr/Ca partitioning. There is little evidence that Sr incorporation into calcite is significantly sensitive to temperature (Huang and Fairchild, 2001), and although Kd_{Mg} is clearly temperature dependent (Gascoyne, 1983; Huang and Fairchild, 2001), it only changes by ~3.7%/°C at 26 °C (Huang and Fairchild, 2001). Between glacial and interglacial times (the largest temperature change likely experienced by the stalagmites), Western-Pacific tropical temperatures warmed by ~2–3.5 °C (Lea, 2000; Rosenthal et al., 2003; Visser et al., 2003; Kienast et al., 2006), so the total change in Mg would be at most 15% compared with the ~300% change observed. The peaks in the Guam speleothem and the spread of Mg values within the different Pacific speleothems are therefore too large to be caused by temperature. We can similarly exclude growth rate as a possible mechanism. Strontium partitioning into calcite is sensitive to growth rate (Mucci and Morse, 1983; Tesorio and Pankow, 1996; Huang and Fairchild, 2001). However, D_{Sr} changes by 15% (Huang and Fairchild, 2001) to 30% (Tesorio and Pankow, 1996) for an order of magnitude change in growth rate. In the Guam speleothem, growth rate changes by at most a factor of 5 (Sinclair et al., in preparation) which is too small to account for the change in Sr. We therefore conclude that the primary changes in Sr/Ca and Mg/Ca in the speleothems must be driven by changing drip water chemistry. Gascoyne (1992), Goede (1994) and Roberts et al. (1999) all report similar conclusions.

Nonetheless, it is possible that temperature plays a secondary role in fractionating Mg. Ku and Li (1998) investigated the use of Mg/Sr ratios as a proxy for temperature, reasoning that if Mg is temperature dependent and Sr is not, then normalising Mg to Sr could remove the influence of changing dripwater chemistry. When we graph the Mg/Sr ratio for the Guam speleothem (Fig. 4c) we find a broad increase beginning between 13 and 15 ka, which could plausibly represent postglacial warming. The Mg/Sr ratio changes by around 100% which is still larger than might be expected based solely on the temperature dependence for Kd_{Mg}. However, our change is similar in magnitude to cycles (reportedly temperature) observed by Ku and Li (1998) suggesting that the temperature dependence of this proxy might be larger than implied by inorganic experiments. Mg/Sr ratios merit further investigation.

4.3.2. Dust and detrital material

We rule out detrital contaminants as a likely source of the Mg and Sr variations. The Pacific islands potentially receive dust from the Gobi desert (Ginoux et al., 2004) and volcanic ash from as far away as Hawaii. Low lying caves (e.g. the Guam site) could also receive winnowed fines (mostly aragonite) from beach sands that dissolve in the re-charge zone for the cave. Dust has been noted as a significant source of Sr in some speleothems (Goede et al., 1998), and clays can also be enriched in Mg (Spivack et al., 1987; Leeman and Sisson, 1996). The elevated Mg and Sr in the Guam speleothem coincide with a region of elevated porosity and ^{232}Th (assumed detrital) (Fig. 4f), consistent with dust as a mechanism for the Mg and Sr correlation.

There is, however, no particular reason why dust input would produce a correlation with the same slope as calcite–water interaction, and it would imply a remarkable coincidence if it were the case. For example, aragonitic beach-dust would result in a much steeper

slope than observed because it is enriched in Sr and depleted in Mg. In addition, we can specifically rule out dust in the more enriched speleothems based on mass balance calculations. The most enriched samples contain up to 2 wt.% Mg, while the Guam speleothem has between ~0.2 and 0.7 wt.% Mg. In order to contain sufficient labile Mg to produce these enrichments, the speleothems would need to contain between 30 wt.% (for Guam) and 70 wt.% clay (assuming the detrital source is smectite which has one of the highest ion absorption capacities of any clay – around 765 meq/kg – Neal, 1977). No observable detrital material was present during sample dissolution.

4.3.3. Soils

Soils play a complex, but potentially important role in setting the Mg and Sr 'starting point' of karst groundwaters. Fairchild and Treble (2009) note that Mg and Sr are normally derived primarily from the carbonate bedrock, possibly excepting where abundant clay minerals are present in the overlying soils. Karmann et al. (2007) show that the Mg and Sr content of drips in the Santana-Pérolas cave system (Brazil) are related to the bulk limestone composition suggesting that the host rock, rather than the soil, plays a dominant role in controlling the overall Mg and Sr composition of groundwaters. However, in that study, soil waters acquired a significant fraction of the Mg and Sr concentrations seen in dripwaters by the time they reached the epikarst zone (Karmann et al., 2007). Similarly, Sr isotope studies in the Edwards Aquifer (Texas) show that soils provide a significant component of radiogenic Sr to vadose cave dripwaters (Musgrove and Banner, 2004). Thus it is possible that the Sr/Ca vs Mg/Ca trend seen for the suite of Pacific speleothems derives from a systematic variation in the composition of the soils overlying the different caves.

Unfortunately, there is insufficient information about soil types in these remote locations to quantitatively test possible soil-based mechanisms. Given the diversity of factors potentially affecting soil composition and leaching, however, it seems unlikely that this could generate one coherent trend between disparate locations, and highly coincidental that this trend should match that predicted by calcite–water interaction.

4.3.4. Sea spray

In an island karst system, input of seawater to groundwaters through sea-spray can be a significant source of ions, especially for Mg and Sr which are both relatively concentrated in seawater (Goede et al., 1998). For example, Fairchild et al. (2000) inferred significant seawater input into one of their cave dripwater systems based on concentrations and ion ratios. Mixing between two waters results in a straight-line correlation between Sr/Ca vs Mg/Ca, connecting the two endmembers (see Appendix B). The mathematics of seawater mixing does not, however, support a straight line in ln(Sr/Ca) vs ln(Mg/Ca) plots, nor does it produce a slope of 0.88. Thus seawater mixing cannot be responsible for the trend seen between the suite of Pacific speleothems. Furthermore, there is no correlation between Mg or Sr and cave-altitude or proximity to the coast, which might be predicted for a sea-spray mechanism.

While seawater mixing could potentially explain the Sr/Ca vs Mg/Ca correlation in the Guam speleothem (Fig. 8), we calculate that dripwaters would need to contain 1.1%–1.8% seawater in order to account for the peak in Mg (Table 6). This is very large compared with typical seawater proportions in rainwater which are in the low sub-% level (calculated using data in Selbu and Steinnes (1995); Reynolds et al. (1997); Campos et al. (2007)). Cation ratios in Jinapsan Cave dripwaters do not support this concentration of seawater (Ca, Mg, and Sr measurements in Partin et al., 2011, Na numbers unpublished). It is possible, however, that sea-spray contributes a second-order effect to the element profiles. During the deglaciation, Jinapsan cave went from ~130 m above sea level to only 25 m. An increasing input of seawater (which is very enriched in Mg relative to Sr) may explain the increasing Mg/Sr in the stalagmite from about 14 ka to present (Fig. 4c).

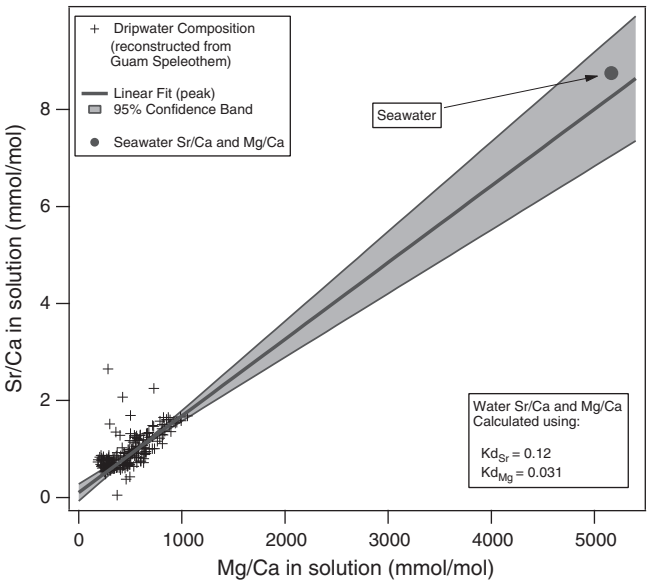

Fig. 8. Sr/Ca vs Mg/Ca mixing between seawater and reconstructed Guam dripwater. Dripwater composition was reconstructed using $Kd_{Sr} = 0.12$ and $Kd_{Mg} = 0.031$ (which is close to our 'preferred' values — see Table 5). Theory predicts a straight line mixing relationship between two water endmembers. The dot indicates the Sr/Ca and Mg/Ca ratios for a pure seawater endmember (taken from Pilson, 1998). This value falls close the linear fit to the reconstructed dripwater data, suggesting that the changes in Mg and Sr in the Guam speleothem could be caused by a changing contribution of seawater to the karst waters.

4.4. Summary

The magnitude of Mg and Sr change seen in our speleothems rules out temperature, growth rate and detrital phases as the mechanism responsible for the trend in Fig. 3. We eliminate seawater input due to a lack of correlation between speleothem Mg + Sr and altitude, and dripwater measurements in the case of the Guam stalagmite. We rule out limestone diagenesis in both the Guam and Pacific speleothems because there is no correlation between Mg or Sr with limestone age, and theoretical considerations do not reproduce the observed linear trend or slope in ln(Sr/Ca) vs ln(Mg/Ca) plots. Soils remain an untested potential source of Mg and Sr variations across the Pacific speleothems but their diverse chemistry makes it unlikely that they would produce a single trend between different sites. The mechanisms offering the best explanation for our observations are 1) prior calcite precipitation (PCP) and 2) incongruent calcite dissolution (ICD).

Thus we conclude that dripwater modification, not host-rock diagenesis, is responsible for the primary Sr/Ca and Mg/Ca cofractionation within the suite of Pacific speleothems. The corollary is that in order for all the different specimens to plot along the same Mg and Sr trend, each of the independent dripwater systems must have had a similar 'starting point' (i.e. initial Mg + Sr composition) presumably imparted from the host rock. Although this seems coincidental given the geographically isolated karst systems, most of the speleothems formed within late Quaternary coral reef limestones that are old enough for unstable mineral assemblages to have mostly been replaced with calcite. This common origin may have imparted a broadly similar Mg and Sr composition to the different limestones.

4.5. Application of models for diagnosis of mechanisms

Our models predict that both PCP and ICD will produce dripwaters or speleothems where plots of ln(Sr/Ca) vs ln(Mg/Ca) have a slope given by $\frac{Kd_{Sr}-1}{Kd_{Mg}-1}$ (calculated to be ~0.88–0.97). While this plot alone cannot distinguish between the mechanisms, they are both facets of 'calcite–water interaction', and both imply that Mg and Sr variations are under hydrological control. In speleothems this would indicate that Mg and Sr could potentially find use as rainfall proxies.

The global nature of this correlation slope, and its insensitivity to host rock and solution composition make it a very useful diagnostic tool for PCP/ICD. To demonstrate, we analyse the data of Wong et al. (2011), who used comprehensive time series of dripwater elemental and isotopic compositions, drip rate, cave-air CO_2, and calcite growth on substrates to classify drips in a central Texas cave into 3 groups. A distinct geochemical evolution mechanism was assigned by Wong et al. (2011) for each group, and we test those assignments using our model. Group 1 drips were mostly driven by PCP, Group 2 and 3 drips were additionally affected by varying degrees of 'water–rock interaction' (equivalent to the processes we identify as 'calcite recrystallization' in Section 4.2.2.). We have graphed the data of Wong et al. (2011) on a ln(Sr/Ca) vs ln(Mg/Ca) plot (Fig. 9), and it is evident that the Group 1 data plot with the slope that is identical to PCP (0.87 ± 0.03) while the Group 3 drips have significantly shallower slopes (0.67 ± 0.03) (see Table 3); consistent with varying degrees of calcite recrystallization. Although the ln(Sr/Ca) vs ln(Mg/Ca) plot does not have the diagnostic utility of a full dripwater analysis program, it nevertheless allows us to distinguish drips experiencing pure PCP from drips experiencing other processes (in this case calcite–water interaction). Speleothems forming from these drips could likewise be characterised, without any additional information about the system. In another example, Griffiths et al. (2010) propose that the correlated Sr/Ca vs Mg/Ca variations in their specimen result from PCP. However, when graphed as ln(Sr/Ca) vs ln(Mg/Ca), the correlation slope is variable but generally significantly steeper than 0.88 (Table 3). This is not consistent with a PCP mechanism.

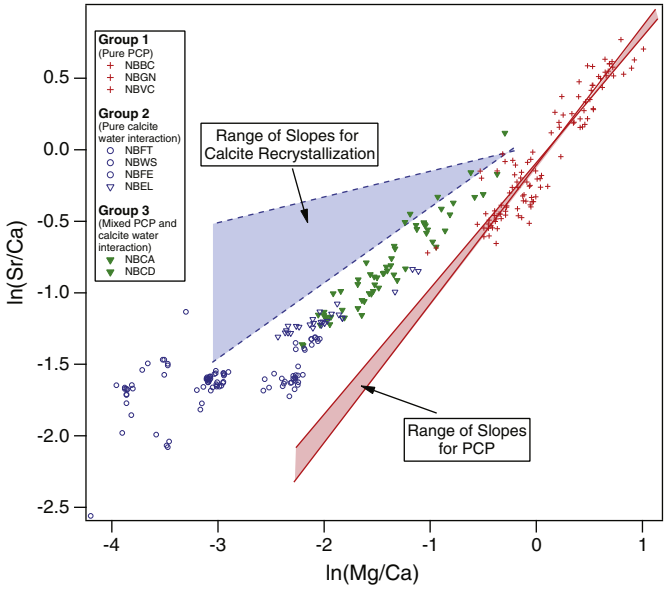

Fig. 9. Drip water data from Natural Bridge Caverns (Wong et al., 2011) graphed as ln(Sr/Ca) vs ln(Mg/Ca). See Wong et al. for drip site abbreviations. Crosses = 'Group 1' drips (identified as pure PCP drip systems). Closed triangles = 'Group 3' drips (identified as being mixed PCP and 'water–rock interaction'). Open symbols = 'Group 2' drips (little or no PCP). Open triangles belong to drip system 'NBEL' which has a composition closest to Group 3 (C. Wong, private communication 2011). Solid lines and shaded area are the range of slopes for our models of PCP/ICD. Dashed lines and shaded area are the range of slopes predicted for our models of calcite recrystallization. Note that the slope of the Group 1 drips is within error of the PCP/ICD slopes (see Table 3), while the slope of the Group 3 drips is shallower and lies between the slopes for calcite recrystallization and PCP (Table 3).

4.6. Interpreting the Guam Mg/Ca and Sr/Ca profiles

Ultimately we aim to use the Mg/Ca and Sr/Ca profiles in the Guam speleothem for paleoenvironmental reconstruction. Having determined that it carries a signature of calcite–water interaction (either PCP or ICD), we now examine the implication this has for changes within the karst system. We do not present a paleoenvironmental story here; this will be considered in greater detail in another paper where we examine the trace element profiles in the context of $\delta^{18}O$ variations in the same speleothem.

From our data alone, we cannot resolve if the peak in Mg/Ca and Sr/Ca during the mid Holocene (Fig. 4a, b) is caused by PCP or ICD. However, Partin et al. (2011) present a dripwater study in Jinapsan Cave showing that Mg/Ca and Sr/Ca increase during summer, coincident with a decrease in Ca, which is diagnostic for PCP. An increase in PCP is typically interpreted as dry conditions (Fairchild et al., 2000; Treble et al., 2003; McMillan et al., 2005; Cruz et al., 2007); however, Tooth and Fairchild (2003) observed elevated Mg/Ca and Sr/Ca during *increased* flow at one of their sites. They interpreted this as a piston-flow mechanism where high infiltration rates displaced a static reservoir of water that had previously undergone PCP. We cannot exclude the possibility that a similar mechanism occurs at our site, although high annual rainfall in the tropics and porous reef limestone make a static reservoir unlikely. We therefore favour the explanation that the Mg and Sr peak in our speleothem represent reduced rainfall during the mid Holocene.

5. Conclusions

- In a suite of Pacific speleothems (from Guam, Vanuatu and the Solomon Islands), the bulk average Sr/Ca and Mg/Ca compositions are positively correlated even though correlations do not exist within all the individual speleothems. On a graph of ln(Sr/Ca) vs ln(Mg/Ca), the data fall on a line with a correlation slope of 0.85 ± 0.14. A high-resolution dataset from one of these speleothems (from Guam), shows a broad peak in Mg/Ca and Sr/Ca which is linear in ln(Sr/Ca) vs ln(Mg/Ca) plots and has a correlation slope of 0.96 ± 0.16. The similarity between these two slopes suggests that the same mechanism may be responsible for partitioning Mg and Sr, and that this mechanism operates over a wide geographic range.
- We eliminate temperature, growth rate, sea-spray and detrital contamination as possible causes of the correlated trend in Mg and Sr. We also eliminate diagenesis: calculations of the dissolution of unstable minerals, and mathematical models of calcite recrystallization, both fail to reproduce the linear correlation or the slope. We investigate whether the correlation could arise through the modification of dripwaters by calcite–water interactions. Two mechanisms are considered: prior calcite precipitation (PCP) and incongruent calcite dissolution (ICD). Mathematical models of PCP predict that it should result in a straight line correlation between ln(Sr/Ca) and ln(Mg/Ca) with a slope given by $\frac{Kd_{Sr}-1}{Kd_{Mg}-1}$. Models of ICD presented in a companion paper (Sinclair, 2011) also predict that a linear correlation with the same slope is possible under conditions that could prevail in the karst. Using published values of Kd_{Sr} and Kd_{Mg}, this correlation slope is calculated to be between 0.88 and 0.97, which is within error of the slopes observed for the speleothems. We therefore conclude that calcite–water interaction is the most likely explanation for the linear ln(Sr/Ca) vs ln(Mg/Ca) trends seen in the Pacific speleothems.

- This mathematical treatment of PCP/ICD proves that the slope depends only on the partition coefficients. It is therefore universal and independent of host-rock or dripwater composition, and has only a minor sensitivity to growth rate. Thus it can be confidently used to identify calcite–water interaction in any cave or dripwater system. In speleothems, this property could be especially useful for diagnosing hydrological control over Mg and Sr partitioning (making them candidates for rainfall reconstruction) *even when no dripwater or bedrock composition is known*.
- We conclude that modification of dripwaters imposes the primary control over the average Mg/Ca and Sr/Ca of the specimens investigated. The other mechanisms identified may also be occurring, responsible for secondary variations such as deviations from the general trend and/or a lack of Mg vs Sr correlation within individual specimens.
- In the Guam stalagmite, drip water data (Partin et al., 2011) supports PCP as the mechanism driving the major Mg and Sr changes. We interpret the mid-Holocene Sr/Ca and Mg/Ca peaks as a hydrological change most likely representing dry conditions in Guam.

Acknowledgments

We wish to thank the Solomon Islands Department of Mines for logistical support during fieldwork, especially Alison Papabatu and Thomas Toba. Michael Rahe is thanked for his help, and we are very grateful to Chief Patrick Manele of Vuranimala Village who accompanied us and provided access to Selwyn's Cave in the Florida Islands (Nggele Pile Island). We are also grateful for the support of people from the Vanuatu Department of Lands and Water: Esline Garaebiti, David Nakadau, Morris Harrison, and Peter Lulu. Rufino Pineda is gratefully acknowledged for providing information on caves in Vanuatu.

We are also grateful to Tom Ada and his family for introducing us to Jinapsan Cave, and the Guam National Wildlife Refuge for providing us access to the Jinapsan Cave, Curt Wexel, Danko Taborosi, Monty Keel and Rob MacCracken for assisting in surveying the cave and in finding and collecting the samples. L. Mack, J. Landrum, L. Heister, T. Housh, G. Thompson, E. James and the UTexas CT facility are thanked for assistance with preparing and analysing samples. M.L. Musgrove, L. Christian, A. Tudhope, T. Crowley, M. Elliot and H. G. Siegrist are also gratefully acknowledged for discussion and ideas which significantly improved this work. This research was partly supported by NSF Marine Geology and Geophysics grant OCE-0402349 to F. Taylor, Jackson School Initiative Program #7 grant to F. Taylor and J. Banner, The Jackson School of Geosciences, and the Geology Foundation and Environmental Science Institute of the University of Texas. Funding for the fieldwork on Guam was generously provided through WERI by the Guam Hydrologic Survey. D. Sinclair wishes to acknowledge financial support from the Scottish Alliance for Geoscience Environment and Society (SAGES) and R. Sherrell (IMCS, Rutgers University). We are grateful to Associate Editor Joel Blum for handling this manuscript and for comments from three anonymous reviewers which improved this work.

Appendix A. Supplementary data

Supplementary data to this article can be found online at doi:10.1016/j.chemgeo.2011.10.008.

References

Banner, J.L., 1995. Application of the trace element and isotope geochemistry of strontium to studies of carbonate diagenesis. Sedimentology 42, 805–824.

Bar-Matthews, M., Ayalon, A., Matthews, A., Sass, E., Halicz, L., 1996. Carbon and oxygen isotope study of the active water-carbonate system in a karstic Mediterranean cave: Implications for paleoclimate research in semiarid regions. Geochimica et Cosmochimica Acta 60 (2), 337–347.

Borsato, A., Frisia, S., Fairchild, I.J., Somogyi, A., Susini, J., 2007. Trace element distribution in annual stalagmite laminae mapped by micrometer-resolution X-ray fluorescence: Implications for incorporation of environmentally significant species. Geochimica et Cosmochimica Acta 71, 1494–1512.

Buhl, D., Immenhauser, A.G.S., Kabiri, L., Richter, D.K., 2007. Time series δ^{26}Mg analysis in speleothem calcite: Kinetic versus equilibrium fractionation, comparison with other proxies and implications for palaeoclimate research. Chemical Geology 244, 715–729.

Campos, V., Costa, A.C.A., Tavares, T.M., 2007. Partial neutralization of rain by seaspray: The case of Recôncavo, Bahia — Brazil. Journal of Environmental Management 84, 204–212.

Carpenter, S.J., Lohmann, K.C., 1992. δ^{18}O values, ^{87}Sr/^{86}Sr and Sr/Mg ratios of modern marine calcite: empirical indicators of ocean chemistry and precipitation rate. Geochimica et Cosmochimica Acta 56 (5), 1837–1849.

Chen, M.-C., Frohlich, C., Taylor, F.W., Burr, G.S., Quarles van Ufford, A., 2011. Arc segmentation and seismicity in the Solomon Island Arc, SW Pacific. : *Tectonophysics*, 507, 47–69.

Cruz Jr., F.W., Burns, S.J., Jercinovic, M., Karmann, I., Sharp, W.D., Vuille, M., 2007. Evidence of rainfall variations in Southern Brazil from trace element ratios (Mg/Ca and Sr/Ca) in a late Pleistocene stalagmite. Geochimica et Cosmochimica Acta 71, 2250–2263.

de Villiers, S., Greaves, M., Elderfield, H., 2002. An intensity ratio calibration method for the accurate determination of Mg/Ca and Sr/Ca of marine carbonates by ICP–AES. Geochemistry, Geophysics, Geosystems 3. doi:10.1029/2001GC000169.

Desmarchelier, J.M., Hellstrom, J.C., McCulloch, M.T., 2006. Rapid trace element analysis of speleothems by ELA-ICP-MS. Chemical Geology 231, 102–117.

Elderfield, H., Bertram, C.J., Erez, J., 1996. A biomineralization model for the incorporation of trace elements into foraminiferal calcium carbonate. Earth and Planetary Science Letters 142, 409–423.

Esat, T.M., McCulloch, M.T., Chappell, J., Pillans, B., Omura, A., 1999. Rapid fluctuations in sea level recorded at Huon Peninsula during the Penultimate deglaciation. Science 283 (5399), 197–201.

Fairchild, I.J., Killawee, J.A., 1995. Selective leaching in glacierized terrains and implications for retention of primary chemical signals in carbonate rocks. In: Kharaka, Y., Chudaev, O.V. (Eds.), Proceedings of the 8th International Symposium on Water/Rock Interactions, Vladivostok, Russia. A. A. Balkema, pp. 79–82.

Fairchild, I.J., Treble, P., 2009. Trace elements in speleothems as recorders of environmental change. Quaternary Science Reviews 28, 449–468.

Fairchild, I.J., Bradby, L., Sharp, M., Tison, J.-L., 1994. Hydrochemistry of carbonate terrains in alpine glacial settings. Earth Surface Processes and Landforms 19 (1), 33–54.

Fairchild, I.J., Killawee, J.A., Sharp, M.J., Spiro, B., Hubbard, B., Lorrain, R.D., Tison, J.-L., 1999. Solute generation and transfer from a chemically reactive alpine glacial-proglacial system. Earth Surface Processes and Landforms 24 (13), 1189–1211.

Fairchild, I.J., Borsato, A., Tooth, A.F., Frisia, S., Hawkesworth, C.J., Huang, Y., McDermott, F., Spiro, B., 2000. Controls on trace element (Sr–Mg) compositions of carbonate cave waters: implications for speleothem climatic records. Chemical Geology 166, 255–269.

Fairchild, I.J., Baker, A., Borsato, A., Frisia, S., Hinton, R.W., McDermott, F., Tooth, A.F., 2001. Annual to sub-annual resolution of multiple trace-element trends in speleothems. Journal of the Geological Society of London 158, 831–841.

Fairchild, I.J., Smith, C.L., Baker, A., Fuller, L., Spötl, C., Mattey, D., McDermott, F., EIMF, 2006a. Modification and preservation of environmental signals in speleothems. Earth-Science Reviews 75, 105–153.

Fairchild, I.J., Tuckwell, G.W., Baker, A., Tooth, A.F., 2006b. Modelling of dripwater hydrology and hydrogeochemistry in a weakly karstified aquifer (Bath, UK): Implications for climate change studies. Journal of Hydrology 321, 213–231.

Finch, A.A., Shaw, P.A., Weedon, G.P., Holmgren, K., 2001. Trace element variation in speleothem aragonite: potential for palaeoenvironmental reconstruction. Earth and Planetary Science Letters 186, 255–267.

Frisia, S., Borsato, A., Fairchild, I.J., Longinelli, A., 1997. Aragontie precipitation at Grotte de Clamouse (Herault, France): role of magnesium and driprate. Proceedings of the 12th International Congress on Speleology, pp. 247–250.

Gagnon, A.C., Adkins, J.F., Fernandez, D.P., Robinson, L.F., 2007. Sr/Ca and Mg/Ca vital effects correlated with skeletal architecture in a scleractinian deep-sea coral and the role of Rayleigh fractionation. Earth and Planetary Science Letters 261 (1–2), 280–295.

Gascoyne, M., 1983. Trace-element partition coefficients in the calcite–water system and their paleoclimatic significance in cave studies. Journal of Hydrology 61, 213–222.

Gascoyne, M., 1992. Palaeoclimate determination from cave calcite deposits. Quaternary Science Reviews 11, 609–632.

Ginoux, P., Prospero, J.M., Torres, O., Chin, M., 2004. Long-term simulation of global dust distribution with the GOCART model: correlation with North Atlantic Oscillation. Environmental Modelling & Software 19 (2), 113–128.

Goede, A., 1994. Continuous early last glacial palaeoenvironmental record from a Tasmanian speleothem based on stable isotope and minor element variations. Quaternary Science Reviews 13, 283–291.

Goede, A., McCulloch, M., McDermott, F., Hawkesworth, C.J., 1998. Aeolian contribution to strontium and strontium isotope variations in a Tasmanian speleothem. Chemical Geology 149, 37–50.

Griffiths, M.L., Drysdale, R.N., Gagan, M.K., Frisia, S., Zhao, J.-x, Ayliffe, L.K., Hantoro, W.S., Hellstrom, J.C., Fischer, M.J., Feng, Y.-X., Suwargadi, B.W., 2010. Evidence for Holocene changes in Australian–Indonesian monsoon rainfall from stalagmite trace element and stable isotope ratios. Earth and Planetary Science Letters 292 (1–2), 27–38.

Hellstrom, J., 2003. Rapid and accurate U/Th dating using parallel ion-counting multi-collector ICP-MS. Journal of Analytical Atomic Spectrometry 18, 1346–1351.

Hellstrom, J., McCulloch, M.T., 2000. Multi-proxy constraints on the climatic significance of trace element records from a New Zealand speleothem. Earth and Planetary Science Letters 179, 287–297.

Hendy, C.H., 1971. The isotopic geochemistry of speleothems — I. The calculation of the effects of different modes of formation on the isotopic composition of speleothems and their applicability as palaeoclimatic indicators. Geochimica et Cosmochimica Acta 35 (8), 801–824.
Holland, H.D., Kirsipu, T.V., Heubner, J.S., Oxburgh, U.M., 1964. On some aspects of the chemical evolution of cave waters. Journal of Geology 72, 36–67.
Howson, M.R., Pethybridge, A.D., House, W.A., 1987. Synthesis and distribution coefficient of low-magnesium calcites. Chemical Geology 64 (1–2), 79–87.
Huang, Y., Fairchild, I.J., 2001. Partitioning of Sr^{2+} and Mg^{2+} into calcite under karst-analogue experimental conditions. Geochimica et Cosmochimica Acta 65 (1), 47–62.
Huang, Y., Fairchild, I.J., Borsato, A., Frisia, S., Cassidy, N.J., McDermott, F., Hawkesworth, C.J., 2001. Seasonal variations in Sr, Mg and P in modern speleothems (Grotta di Ernesto, Italy). Chemical Geology 175, 429–448.
Hughes, G.W., 1989. The Micropaleontology of sedimentary units from the Solomon Islands. In: Vedder, J.G., Bruns, T.R. (Eds.), Circum-Pacific Council for Energy and Mineral Resources Earth Science Series. : Geology and Offshore Resources of Pacific Island Arcs, 12. Solomon Islands and Bougainville, Papua New Guinea Regions, pp. 227–237.
Johnson, K.R., Hu, C., Belshaw, N.S., Henderson, G.M., 2006. Seasonal trace-element and stable-isotope variations in a Chinese speleothem: the potential for high-resolution paleomonsoon reconstruction. Earth and Planetary Science Letters 244 (1–2), 394–407.
Karmann, I., Cruz Jr., F.W., Oduvaldo, V.J., Burns, S.J., 2007. Climate influence on geochemistry parameters of waters from Santana–Pérolas cave system, Brazil. Chemical Geology 244, 232–247.
Kienast, M., Kienast, S.S., Calvert, S.E., Eglinton, T.I., Mollenhauer, G., Francois, R., Mix, A.C., 2006. Eastern Pacific cooling and Atlantic overturning circulation during the last deglaciation. Nature 443 (7113), 846–849.
Ku, T.L., Li, H.C., 1998. Speleothems as high-resolution paleoenvironment archives: records from northeastern China. Proceedings of the Indian Academy of Science 107 (4), 321–330.
Land, L.S., 1967. Diagenesis of skeletal carbonates. Journal of Sedimentary Petrology 37 (3), 914–930.
Lea, D.W., 2000. Climate impact of late quaternary equatorial Pacific sea surface temperature variations. Science 289, 1719–1724.
Leeman, W.P., Sisson, V.B., 1996. Geochemistry of boron and its implications for crustal and mantle processes. In: Grew, E.S., Anovitz, L.M. (Eds.), Boron: Mineralogy, Petrology and Geochemistry in the Earth's Crust: Mineralogical Society of America, Vol. 33, pp. 645–707.
Mattey, D., Lowry, D., Duffet, J., Fisher, R., Hodge, E., Frisia, S., 2008. A 53 year seasonally resolved oxygen and carbon isotope record from a modern Gibraltar speleothem: Reconstructed drip water and relationship to local precipitation. Earth and Planetary Science Letters 269, 80–95.
McDonald, J., Drysdale, R.N., Hill, D., 2004. The 2002–2003 El Niño recorded in Australian cave drip waters: implications for reconstructing rainfall histories using stalagmites. Geophysical Research Letters 31, L22202. doi:10.1029/2004GL020859.
McGillen, M.R., Fairchild, I.J., 2005. An experimental study of incongruent dissolution of $CaCO_3$ under analogue glacial conditions. Journal of Glaciology 51 (174), 383–390.
McMillan, E.A., Fairchild, I.J., Frisia, S., Borsato, A., McDermott, F., 2005. Annual trace element cycles in calcite–aragonite speleothems: evidence of drought in the western Mediterranean 1200–1100 yr BP. Journal of Quaternary Science 20 (5), 423–433.
Mickler, P.J., Banner, J.L., Stern, L., Asmerom, Y., Edwards, R.L., Ito, E., 2004. Stable isotope variations in modern tropical speleothems: Evaluating equilibrium vs. kinetic isotope effects. Geochimica et Cosmochimica Acta 68 (21), 4381–4393.
Miklavič, B., 2011. Formation of Geomorphic Features as a Response to Sea-level Change at Ritidian Point. Mariana Islands, Guam. Masters thesis, Mississippi State University, Available online at http://sun.library.msstate.edu/ETD-db/theses/available/etd-03262011-212710/.
Moore, C.H., 2001. Developments in Sedimentology 55: Carbonate Reservoirs — Porosity Evolution and Diagenesis in a Sequence Stratigraphic Framework. Elsevier.
Morse, J.W., Mackenzie, F.T., 1990. Geochemistry of Sedimentary Carbonates. Elsevier.
Mucci, A., Morse, J.W., 1983. The incorporation of Mg^{2+} and Sr^{2+} into calcite overgrowths: influences of growth rate and solution composition. Geochimica et Cosmochimica Acta 47 (2), 217–233.
Musgrove, M., Banner, J.L., 2004. Controls on the spatial and temporal variability of vadose dripwater geochemistry: Edwards Aquifer, central Texas. Geochimica et Cosmochimica Acta 68 (5), 1007–1020.
Neal, C., 1977. The determination of adsorbed Na, K, Mg and Ca on sediments containing $CaCO_3$ and $MgCO_3$. Clays and Clay Minerals 25, 253–258.
Paquette, J., Reeder, R.J., 1995. Relationship between surface structure, growth mechanism, and trace element incorporation in calcite. Geochimica et Cosmochimica Acta 59 (4), 735–749.
Partin J. W., Jenson J. W., Banner J. L., Quinn T. M., Taylor F. W., Sinclair D., Hardt B., Lander M., Bell T., Miklavič B., Jocson J.M., and Taborosi D. (2011) Relationship between modern rainfall variability, cave dripwater and stalagmite geochemistry in Guam, USA. Geochemistry, Geophysics, Geosystems (in review).
Pilson, M.E.Q., 1998. An Introduction to the Chemistry of the Sea. Prentice Hall.
Quinn, T.M., 1991. Meteoric diagenesis of Plio-Pleistocene limestones at Enewetak Atoll. Journal of Sedimentary Research 61 (5), 681–703.
Reeve, A.S., Perry, E.C., 1994. Carbonate geochemistry and the concentrations of aqueous Mg^{2+}, Sr^{2+} and Ca^{2+}: western north coast of the Yucatan, Mexico. Chemical Geology 112, 105–117.
Reynolds, B., Fowler, D., Smith, R.I., Hall, J.R., 1997. Atmospheric inputs and catchment solute fluxes for major ions in five Welsh upland catchments. Journal of Hydrology 194, 305–329.
Ristvet, B.L., 1971. The progressive diagenetic history of Bermuda. Bermuda Biological Station for Research Special Publication 9, 118–157.
Roberts, M.S., Smart, P.L., Baker, A., 1998. Annual trace element variations in a Holocene speleothem. Earth and Planetary Science Letters 154, 237–246.
Roberts, M.S., Smart, P.L., Hawkesworth, C.J., Perkins, W.T., Pearce, N.J.G., 1999. Trace element variations in coeval Holocene speleothems from GB Cave, southwest England. The Holocene 9 (6), 707–713.
Rosenthal, Y., Oppo, D.W., Linsley, B.K., 2003. The amplitude and phasing of climate change during the last deglaciation in the Sulu Sea, western equatorial Pacific. Geophysical Research Letters 30 (8), 1428.
Schmidt, G.A., LeGrande, A.N., Hoffmann, G., 2007. Water isotope expressions of intrinsic and forced variability in a coupled ocean–atmosphere model. Journal of Geophysical Research 112. doi:10.1029/2006JD007781.
Schrag, D.P., 1999. Rapid analysis of high-precision Sr/Ca ratios in corals and other marine carbonates. Paleoceanography 14 (2), 97–102.
Schroeder, J.H., 1969. Experimental dissolution of calcium, magnesium, and strontium from recent biogenic carbonates: a model of diagenesis. Journal of Sedimentary Petrology 39 (3), 1057–1073.
Selbu, B., Steinnes, E., 1995. Trace Elements in Natural Waters. CRC Press.
Sinclair, D.J., 2011. Two mathematical models of Mg and Sr partitioning into solution during incongruent calcite dissolution. Application to karst and speleothem studies. Chemical Geology 283 (3–4), 119–133.
Sinclair, D.J., Kinsley, L.P.J., McCulloch, M.T., 1998. High resolution analysis of trace elements in corals by laser-ablation ICP-MS. Geochimica et Cosmochimica Acta 62 (11), 1889–1901.
Sinclair, D.J., Sherwood, O.A., Risk, M.J., Hillaire-Marcel, C., Tubrett, M., Sylvester, P., McCulloch, M.T., Kinsley, L.P.J., 2005. Testing the reproducibility of Mg/Ca profiles in the deep-water coral *Primnoa resedaeformis*: putting the proxy through its paces. In: Freiwald, A., Roberts, J.M. (Eds.), Cold Water Corals and Ecosystems — Selected Papers from the 2nd International Symposium on Deep Sea Corals. Springer-Verlag, pp. 1039–1060.
Sinclair, D.J., Allard, G., Williams, B., Ross, S., Risk, M.J., 2011. Reproducibility of trace element profiles in a specimen of the deep-water bamboo coral keratoisis sp. Geochimica et Cosmochimica Acta 75 (18), 5101–5121.
Sinclair D. J., Partin J. W., Taylor F. W., Banner J. L., Jenson J., Mylroie J., Goddard E., Quinn T., Lander M. A., and Jocson J. (in preparation) Evidence for changes in atmospheric circulation over the Western Pacific during the Early–Mid Holocene: preliminary results from geochemical analysis of a speleothem from Guam.
Spivack, A.J., Palmer, M.R., Edmond, J.M., 1987. The sedimentary cycle of the boron isotopes. Geochimica et Cosmochimica Acta 51, 1939–1949.
Stipp, S.L.S., Gutmannsbauer, W., Lehmann, T., 1996. The dynamic nature of calcite surfaces in air. American Mineralogist 81, 1–8.
Stirling, C.H., Esat, T.M., Lambeck, K., McCulloch, M.T., 1998. Timing and duration of the Last Interglacial: evidence for a restricted interval of widespread coral reef growth. Earth and Planetary Science Letters 160 (3–4), 745–762.
Tatár, E., Mihucz, V.G., Zámbó, L., Gasparics, T., Záray, G., 2004. Seasonal changes of fulvic acid, Ca and Mg concentrations of water samples collected above and in the Béke Cave of the Aggtelek karst system (Hungary). Applied Geochemistry 19, 1727–1733.
Taylor, F.W., Mann, P., Bevis, M.G., Edwards, R.L., Cheng, H., Cutler, K.B., Gray, S.C., Burr, G.S., Beck, J.W., Phillips, D.A., Cabioch, G., Recy, J., 2005. Rapid forearc uplift and subsidence caused by impinging bathymetric features: examples from the New Hebrides and Solomon arcs. Tectonics 24 (6) TC6005.
Tesorio, A.J., Pankow, J.F., 1996. Solid solution partitioning of Sr^{2+}, Ba^{2+}, and Cd^{2+} to calcite. Geochimica et Cosmochimica Acta 60 (6), 1053–1063.
Tooth, A.F., Fairchild, I.J., 2003. Soil and karst aquifer hydrological controls on the geochemical evolution of speleothem-forming drip waters, Crag Cave, southwest Ireland. Journal of Hydrology 273, 51–68.
Treble, P., Shelley, J.M.G., Chappell, J., 2003. Comparison of high resolution sub-annual records of trace elements in a modern (1911–1992) speleothem with instrumental climate data from southwest Australia. Earth and Planetary Science Letters 216, 141–153.
Treble, P., Chappell, J., Shelley, J.M.G., 2005. Complex speleothem growth processes revealed by trace element mapping and scanning electron microscopy of annual layers. Geochimica et Cosmochimica Acta 69 (20), 4855–4863.
Villegas-Jimenez, A., Mucci, A., Paquette, J., 2009. Proton/calcium ion exchange behavior of calcite. Physical Chemistry Chemical Physics 11 (39), 8895–8912.
Visser, K., Thunell, R., Stott, L., 2003. Magnitude and timing of temperature change in the Indo-Pacific warm pool during deglaciation. Nature 421, 152–155.
Wong, C.I., Banner, J.L., Musgrove, M., 2011. Seasonal dripwater Mg/Ca and Sr/Ca variations driven by cave ventilation: implications for and modeling of speleothem paleoclimate records. Geochimica et Cosmochimica Acta 75 (12), 3514–3529.